Functionally, failure of EGFR to correctly localize to cell membrane is expected to reduce ligand binding. In healthy people, several ligands require proteolytic cleavage to become capable of binding to EGFR—this ectodomain shedding is induced by at least five different metalloprotease enzymes, including ADAM17 (Blobel, 2005)—mutations in which may underlie an inflammatory skin and bowel disease that has overlap with the clinical features present in our patient (Blaydon *et al.*, 2011). We hypothesize that the lack of EGFR localization at the cell membrane in our patient has some similarity at a signaling level to that which occurs in the ADAM17-deficient patients, i.e., a common failure of EGFR–ligand interaction and altered downstream signal transduction.

Clinicopathologic similarities with mouse models of EGFR impairment

The clinical manifestations of the mutation p.Gly428Asp in terms of loss of EGFR function show some similarities with the phenotype of *Egfr*-knockout or transgenic mice (Miettinen *et al.*, 1995; Sibilia and Wagner, 1995; Threadgill *et al.*, 1995; Schneider *et al.*, 2008). Although the phenotype of *Egfr*-deficient mice depends on the strain of the mice (several are embryonic lethal), the abnormalities in the skin, lung, and bowel in surviving mice are similar to many of the clinical manifestations in our patient. In the epidermis, some knockout mice show an initially thin skin that then becomes thicker but with defective barrier function (Miettinen *et al.*, 1995). Lack of *Egfr* in mice also affects hair growth, with wavy or reduced hair growth; EGFR is essential for normal hair follicle progression through the anagen, catagen, and telogen phases of the hair growth cycle (Hansen *et al.*, 1997; Schneider *et al.*, 2008). EGFR initiates hair growth and hair follicle organization, and EGFR inhibition leads to inflammation, follicular necrosis, and alopecia, as well as slow hair growth with brittle hairs, as observed in our patient (Hansen *et al.*, 1997; Schneider *et al.*, 2008). *Egfr*-deficient mouse lungs show condensed collapsed alveoli with a lack of surfactant leading to respiratory difficulty that has been likened to human neonatal respiratory distress syndrome (Miettinen *et al.*, 1995). In murine bowel lacking Egfr, there are fewer, shorter intestinal villi, and a reduced proliferation of jejunal enterocytes leading to fluid loss (Miettinen *et al.*, 1995). Other abnormalities noted in the mice that show phenotypic similarities to our patient have included cystic dilatation of the collecting ducts in the kidneys (indicating that EGFR is vital for the differentiation of structures derived from the ureteric bud), aortic narrowing, and a thrombotic tendency (Miettinen *et al.*, 1995). In addition, there are similarities in the phenotype of transgenic *Egfr* and *Adam17* mice, thus supporting the clinical overlap in humans with germline autosomal recessive mutations in *EGFR* or *ADAM17* (Peschon *et al.*, 1998).

Clinical resemblance to the side effects of EGFR inhibitor medications

The clinical manifestations in the child homozygous for p.Gly428Asp in *EGFR* also show some resemblance to the side effect profile in individuals taking EGFR inhibitors. The side effects of these drugs include a distinctive acne-like rash with pustules, dry skin, alopecia, trichomegaly, as well as mucositis, diarrhea, and, in rare instances, interstitial lung disease (Inoue *et al.*, 2003; Lacouture, 2006). All these clinical features were evident to some degree in our patient. Nevertheless, although skin papules and pustules developed during disease progression in our case, the early skin changes mostly consisted of erosions (which led to the erroneous initial clinical diagnosis of epidermolysis bullosa). EGFR signaling is known to be involved in the re-epithelialization phase of wound healing (Repertinger *et al.*, 2004; Pastore *et al.*, 2008), as well as the proliferation of keratinocyte stem cells (Jensen *et al.*, 2009), and we hypothesize that the missense mutation in our patient impeded these processes and was the primary cause of the erosive skin changes, with bacterial superinfection being a secondary contributing factor. The transcriptomic data from our patient illustrate the consequences of impaired EGFR signaling. The results (albeit based on RNA extracted from noninflamed skin) reveal enhanced proinflammatory activation and disturbed differentiation/premature terminal differentiation of keratinocytes as key pathogenic mechanisms, thereby demonstrating a similar profile to that associated with the papulo-pustular rash associated with EGFR inhibitory drugs (Lacouture, 2006; Lichtenberger *et al.*, 2013; Mascia *et al.*, 2013). Notably, several inflammatory/innate response networks were significantly upregulated, including NF-κB.

In conclusion, the EGFR network is one of the most influential and intricate signaling systems in biology. We believe the protean features in our patient offer clinical insights into the critical and diverse roles of EGFR, supporting many of the putative functions that have been ascribed to the receptor via murine models and *in vitro* studies. This case highlights the major mechanism of epithelial dysfunction following EGFR signaling ablation and illustrates the broader impact of EGFR inhibition on other tissues that might be underappreciated in the context of concurrent malignancy in patients receiving EGFR inhibitor medications.

MATERIALS AND METHODS

Transmission electron microscopy

Small pieces of skin (<2 mm^3) were prepared for transmission electron microscopy, as described in the Supplementary Material online.

Immunofluorescence microscopy

A skin biopsy from the affected infant and control skin were collected in Michel's medium. The methods for immunofluorescence microscopy and primary antibodies used are listed in the Supplementary Material online.

Whole-exome sequencing

Initially, 3 μg of genomic DNA was sheared with focused acoustic technology (Covaris, Woburn, MA) to yield a mean fragment size of 150 bp. Fragment ends were repaired and sequencing adaptors ligated. Biotinylated 120 bp RNA probes (Agilent, Santa Clara, CA), designed against the coding regions of the genome were hybridized with the sequence library for 24 hours. DNA bound to RNA probes was retained using streptavidin-coated magnetic beads; unbound DNA was washed off. The exome-enriched pool of DNA was eluted

and amplified with a low-cycle PCR. The DNA fragments were then sequenced with 100 bp paired-end reads. Novoalign (Novocraft Technologies, Selangor, Malaysia) was used to align reads to the reference genome (hg19, National Center for Biotechnology Information build 37). With over 7.0 Gb of sequence generated, more than 90% of coding bases of the GENCODE-defined exome were represented by at least 20 reads (see Supplementary Material online).

Sanger sequencing

We sequenced the exon and intron/exon boundaries of all 28 exons of *EGFR*, including the mutation present in exon 11, in the infant, mother, unaffected older brother, and three controls. Each exon was amplified by PCR using AmpliTaq Gold 360 Master Mix (Applied Biosystems, Foster City, CA) and the primers listed in the Supplementary Material online.

Whole-genome expression microarray analysis

Whole-genome expression microarray analysis was performed using RNA extracted from skin biopsies sampled from the affected child as well as four pooled, healthy controls. RNA extraction from cutaneous biopsies was performed using the Ambion mirVana miRNA Isolation kit (Invitrogen, Paisley, UK) according to the manufacturer's instructions. RNA was amplified using the Illumina TotalPrep RNA Amplification Kit (Illumina) and subsequent gene expression profiling was performed using the Illumina array HumanHT-12 v4.0 Expression BeadChip kit according to the manufacturer's instructions (Illumina). Gene expression data were then analyzed using GenomeStudio software (Illumina). Control samples were pooled and compared with the affected individual.

Mutant construct transfection

Mutant complementary DNA mimicking the mutation of the infant (c.1283G>A) was generated with GFP tagged to the C terminus of EGFR. Wild-type EGFR1-GFP was a gift from Dr Andrew Reynolds (Institute for Cancer Research, London, UK). The mutant construct p.Gly428Asp EGFR-GFP was generated using a site-directed mutagenesis kit (Stratagene, La Jolla, CA) as per the manufacturer's instructions using the following mutagenesis primer: 5′-GAGAACCT AGAAATCATACGCGACAGGACCAAGCAACATGGT-3′. The mutation in the plasmid was verified by sequencing. Transfection was carried out using Fugene (Roche Applied Science, Penzberg, Germany) or Lipofectamine (Invitrogen) reagents according to the manufacturers' instructions.

Confocal microscopy

For confocal microscopy, cultured MCF-7 human breast adenocarcinoma cells were transfected with wild-type EGFR-GFP or p.Gly428Asp EGFR-GFP washed with phosphate-buffered saline, fixed with 4% paraformaldehyde in phosphate-buffered saline for 10 minutes, and then permeabilized with 0.2% TritonX-100 for 10 minutes. For EGF stimulation experiments, cells were incubated in serum-free medium (Opti-MEM; Gibco Life Technologies, Carlsbad, CA) for 16 hours before stimulation with 100 ng ml^{-1} EGF for the indicated times. For endocytosis inhibition experiments, cells were treated for 1 hour with 10 μM Dynasore (Millipore, Billerica, MA) or equivalent volume of DMSO as a control before fixation. Where appropriate, cells were incubated with a primary antibody directed against the extracellular domain of EGFR for 2 hours followed by the relevant secondary antibodies conjugated to Alexafluor-568 (Life Technologies, Paisley, UK) and phalloidin conjugated to Alexafluor-568 or 633 for 1 hour at room temperature.

Western blotting

Thirty thousand MCF-7 or CHO cells per condition were cultured in either DMEM alone or DMEM containing 10% fetal calf serum (10% FCS) and transfected with wild-type EGFR-GFP or p.Gly428Asp EGFR-GFP; 36 hours later, the cells were starved for 16 hours with Opti-MEM (Gibco Life Technologies) before treatment with 100 ng ml^{-1} EGF for the appropriate times. Cells were then lysed in sample buffer containing 2-mercaptoethanol at room temperature. Lysates were immediately subjected to SDS–PAGE and blotted using nitrocellulose membrane. Blots were blocked and probed using p-ERK, ERK, p-Akt, Akt, p-EGFR, and EGFR antibodies (Cell Signaling Technology, Beverly, MA), as well as HSC-70 antibodies (Santa Cruz Biotechnology, Dallas, Texas), using 3% milk/phosphate-buffered saline–0.2% Tween or 5% BSA/TBS-0.1% Tween.

Growth assessment rates

Ten thousand CHO cells per condition were cultured in DMEM containing 10% FCS for 24 hours before transfection with GFP alone, wild-type EGFR-GFP, or p.Gly428Asp EGFR-GFP. Twenty-four hours later, the medium was replaced with normal growth medium (10% FCS), growth medium minus FCS, or growth medium minus FCS supplemented with 100 ng ml^{-1} EGF. Cells were then either Hoechst treated and fixed immediately with 4% paraformaldehyde or were fixed 24 hours later. Phase and Hoechst images of five fields of view per condition were taken using an Olympus IX71 wide-field microscope with a 4 × 0.13 numerical aperture air objective (Olympus, Tokyo, Japan). Images were then analyzed for total number of cells as well as GFP-expressing cells. The number of GFP-expressing cells was then normalized using the total number of cells per field of view and presented either as the average number of GFP-expressing cells per condition or the growth rate per condition.

CONFLICT OF INTEREST

The authors state no conflict of interest.

ACKNOWLEDGMENTS

The Centre for Dermatology and Genetic Medicine is supported by a Wellcome Trust Strategic Award (reference number 098439/Z/12/Z). The work was also supported by the UK National Institute for Health Research (NIHR) Biomedical Research Centre based at Guy's and St Thomas' NHS Foundation Trust and King's College London, as well as DebRA UK, and the British Association of Dermatologists. This study was also supported, in part, by the Great Britain Sasakawa Foundation (award no. 4314) and Strategic Young Researcher Overseas Visits Program for Accelerating Brain Circulation (S2404) from the Japan Society for the Promotion of Science. We also thank Venu Pullabhatla for assistance with transcriptomic data analysis and access.

SUPPLEMENTARY MATERIAL

Supplementary material is linked to the online version of the paper at http://www.nature.com/jid

REFERENCES

Avraham R, Yarden Y (2011) Feedback regulation of EGFR signalling: decision making by early and delayed loops. *Nat Rev Mol Cell Biol* 12:104–17

Adzhubei IA, Schmidt S, Peshkin L *et al.* (2010) A method and server for predicting damaging missense mutations. *Nat Methods* 7:248–9

Blaydon DC, Biancheri P, Di WL *et al.* (2011) Inflammatory skin and bowel disease linked to ADAM17 deletion. *N Engl J Med* 365:1502–8

Blobel CP (2005) ADAMs: key components in EGFR signalling and development. *Nat Rev Mol Cell Biol* 6:32–43

Chavanas S, Bodener C, Rochat A *et al.* (2000) Mutations in SPINK5, encoding a serine protease inhibitor, cause Netherton syndrome. *Nat Genet* 25 141–2

Dawson JP, Berger MB, Lin CC *et al.* (2005) Epidermal growth factor receptor dimerization and activation require ligand-induced conformational changes in the dimer interface. *Mol Cell Biol* 25:7734–42

Dreux AC, Lamb DJ, Modjtahedi H *et al.* (2006) The epidermal growth factor receptors and their family of ligands: Their putative role in atherogenesis. *Atherosclerosis* 186:38–53

Fine JD, Eady RA, Bauer EA *et al.* (2008) The classification of inherited epidermolysis bullosa (EB): report of the third international consensus meeting on diagnosis and classification of EB. *J Am Acad Dermatol* 58:931–50

Gschwind A, Fischer OM, Ullrich A (2004) The discovery of receptor tyrosine kinases: targets for cancer therapy. *Nat Rev Cancer* 4:361–70

Hansen LA, Alexander N, Hogan ME *et al.* (1997) Genetically null mice reveal a central role for epidermal growth factor receptor in the differentiation of the hair follicle and normal hair development. *Am J Pathol* 150:1959–75

Inoue A, Saijo Y, Maemondo M *et al.* (2003) Severe acute interstitial pneumonia and gefitinib. *Lancet* 361:137–9

Jensen KB, Collins CA, Nascimento E *et al.* (2009) Lrig1 expression defines a distinct multipotent stem cell population in mammalian epidermis. *Cell Stem Cell* 4:427–39

Jost M, Kari C, Rodeck U (2000) The EGF receptor - an essential regulator of multiple epidermal functions. *Eur J Dermatol* 10:505–10

Jutten B, Rouschop KM (2014) EGFR signaling and autophagy dependence for growth, survival, and therapy resistance. *Cell Cycle* 13:42–51

Kumar A, Petri ET, Halmos B *et al.* (2008) Structure and clinical relevance of the epidermal growth factor receptor in human cancer. *J Clin Oncol* 26:1742–51

Lacouture ME (2006) Mechanisms of cutaneous toxicities to EGFR inhibitors. *Nat Rev Cancer* 6:803–12

Lee CS, Kim IS, Park JB *et al.* (2006) The phox homology domain of phospholipase D activates dynamin GTPase activity and accelerates EGFR endocytosis. *Nat Cell Biol* 8:477–84

Lichtenberger BM, Gerber PA, Holcmann M *et al.* (2013) Epidermal EGFR controls cutaneous host defense and prevents inflammation. *Sci Transl Med* 5:199ra111

Liu HB, Wu Y, Lv TF *et al.* (2013) Skin rash could predict the response to EGFR tyrosine kinase inhibitor and the prognosis for patients with non-small cell lung cancer: a systematic review and meta-analysis. *PLoS One* 8:e55128

Macia E, Ehrlich M, Massol R *et al.* (2006) Dynasore, a cell-permeable inhibitor of dynamin. *Dev Cell* 10:839–50

Mascia F, Lam G, Keith C *et al.* (2013) Genetic ablation of epidermal EGFR reveals the dynamic origin of adverse effects of anti-EGFR therapy. *Sci Transl Med* 5:199ra110

Miettinen PJ, Berger JE, Meneses J *et al.* (1995) Epithelial immaturity and multiorgan failure in mice lacking epidermal growth factor receptor. *Nature* 376:337–41

Nanba D, Toki F, Barrandon Y *et al.* (2013) Recent advances in the epidermal growth factor/ligand system biology on skin homeostasis and keratinocyte stem cell regulation. *J Dermatol Sci* 72:81–6

Ng PC, Henikoff S (2003) SIFT: predicting amino acid changes that affect protein function. *Nucleic Acids Res* 31:3812–4

Ogiso H, Ishitani R, Nureki O *et al.* (2002) Crystal structure of the complex of human epidermal growth factor and receptor extracellular domains. *Cell* 110:775–87

Perrotte P, Matsumoto T, Inoue K *et al.* (1999) Anti-epidermal growth factor receptor antibody C225 inhibits angiogenesis in human transitional cell carcinoma growing orthotopically in nude mice. *Clin Cancer Res* 5: 257–65

Pastore S, Mascia F, Mariani V *et al.* (2008) The epidermal growth factor receptor system in skin repair and inflammation. *J Invest Dermatol* 128:1365–74

Peschon JJ, Slack JL, Reddy P *et al.* (1998) An essential role for ectodomain shedding in mammalian development. *Science* 282:1281–4

Petrof G, Mellerio JE, McGrath JA (2012) Desmosomal genodermatoses. *Br J Dermatol* 166:36–45

Repertinger SK, Campagnaro E, Fuhrman J *et al.* (2004) EGFR enhances early healing after cutaneous incisional wounding. *J Invest Dermatol* 123: 982–9

Rodeck U, Jost M, Kari C *et al.* (1997) EGF-R dependent regulation of keratinocyte survival. *J Cell Sci* 110:113–21

Schneider MR, Werner S, Paus R *et al.* (2008) Beyond wavy hairs: the epidermal growth factor receptor and its ligands in skin biology and pathology. *Am J Pathol* 173:14–24

Schneider MR, Wolf E (2009) The epidermal growth factor receptor ligands at a glance. *J Cell Physiol* 218:460–6

Sibilia M, Kroismayr R, Lichtenberger BM *et al.* (2007) The epidermal growth factor receptor: from development to tumorigenesis. *Differentiation* 75:770–87

Sibilia M, Wagner EF (1995) Strain-dependent epithelial defects in mice lacking the EGF receptor. *Science* 269:234–8

Stoll C, Alembik Y, Tchomakov D *et al.* (2001) Severe hypernatraemic dehydration in an infant with Netherton syndrome. *Genet Counsel* 12:237–43

Threadgill DW, Dlugosz AA, Hansen LA *et al.* (1995) Targeted disruption of mouse EGF receptor: effect of genetic background on mutant phenotype. *Science* 269:230–4

Zhang Z, Xiao C, Gibson AM *et al.* (2014) EGFR signaling blunts allergen-induced IL-6 production and Th17 responses in the skin and attenuates development and relapse of atopic dermatitis. *J Immunol* 192:859–66

IL36RN Mutations Underlie Impetigo Herpetiformis

Journal of Investigative Dermatology (2014) **134,** 2472–2474; doi:10.1038/jid.2014.177; published online 1 May 2014

TO THE EDITOR

Impetigo herpetiformis (IH) is a rare pustular dermatosis that typically occurs in pregnant women sporadically with unknown etiology (Sauer and Geha, 1961). Early diagnosis is essential, as IH is life-threatening and is associated with placental insufficiency and electrolyte abnormalities. IH appears to have the same clinical and histologic appearance as generalized pustular psoriasis (GPP), which is also a rare severe episodic pustular dermatosis that occurs repeatedly in both sexes at any age. However, some researchers have regarded IH as an entity distinct from GPP, because some patients are affected by IH only in the gestational period (Lotem *et al.*, 1989). Recently, we reported that the majority of GPP that is not accompanied by psoriasis vulgaris (PV; GPP alone) is caused by homozygous or compound heterozygous mutations of *IL36RN*, which encodes IL-36 receptor antagonist (IL-36RN), although only a small number of cases with GPP preceding or accompanied by PV (GPP with PV) were found to have *IL36RN* mutations (Sugiura *et al.*, 2013). Very recently, we reported that *CARD14* c.526G>C is a significant risk factor for GPP with PV, but not for GPP alone in the Japanese cohort, which further supports the idea that GPP with PV differs genetically from GPP alone (Sugiura *et al.*, 2014a). However, to our knowledge, there have been no reports of IH with *IL36RN* mutations. Here we report two cases of IH with homozygous and heterozygous *IL36RN* mutations.

Cases 1 and 2 were a 23-year-old woman and a 28-year-old Japanese woman who were admitted to our hospitals for pustular lesions in the 29th week and the 20th week of their first pregnancies, respectively (Figure 1a and b). There was no family history of GPP, no IH, and no consanguinity in their families. Case 1 had no previous history of GPP. Her pustular lesions had begun to develop at the 21st week of pregnancy, and she had been hospitalized in a maternity hospital. Oral prednisolone at a dose of 15 mg per day had been administered, but the eruptions had persisted. A skin biopsy from a pustular eruption on the trunk revealed a spongiform pustule of Kogoj in the epidermis consistent with IH (Figure 1c). Case 2 had suffered from GPP from the age of 8 to 18 years. Skin biopsies from pustular eruptions on the trunk revealed spongiform pustules of Kogoj in the epidermis at the age of 8 and 28 years (Figure 1d). She had been admitted to hospitals four times for GPP flare-ups. She had been treated with cyclosporine or etretinate. In the ten years leading up to her pregnancy, her GPP had been in remission without any treatment. Both cases had erythema with pustules over the whole body and fever of over 38 °C. Blood examinations from Cases 1 and 2, respectively, revealed white blood cell counts of 12,000 μl^{-1} and 21,170 μl^{-1}, and C-reactive protein concentrations of 6.5 and 14.9 mg dl^{-1} (normal range: <0.3 mg dl^{-1}). Bacterial cultures of the pustules were negative. Thus, Cases 1 and 2 were, respectively, diagnosed as having IH and IH with a previous history of GPP.

Following ethical approval, written informed consent was obtained in compliance with the Declaration of Helsinki Principles. The entire coding regions of *IL36RN* including the exon/intron boundaries were sequenced using genomic DNA samples from the patients. Case 1 had the homozygous mutation c.115+6T>C, which was proven to result in p.Arg10ArgfsX1 in *IL36RN* by us previously, and Case 2 had the heterozygous mutation c.28C>T (p.Arg10X) in *IL36RN*. Both of these are GPP-causing founder mutations in the Japanese cohort (Sugiura *et al.*, 2013, 2014b; Figure 1e and f, and Figure 2). A search for a second *IL36RN* mutation in all intron and putative promoter regions in Case 2 revealed no other *IL36RN* mutations (Supplementary Figure S1 online and Supplementary Table S1 online). However, there is still the possibility of a second unidentified *IL36RN* mutation in Case 2.

More than 10 cases of GPP with heterozygous *IL36RN* mutations have been reported (Capon, 2013; Korber *et al.*, 2013; Li *et al.*, 2013; Setta-Kaffetzi *et al.*, 2013; Sugiura *et al.*, 2013). Moreover, in some patients, heterozygous *IL36RN* mutations are associated with palmoplantar pustulosis, a type of pustular psoriasis, and acute generalized exanthematous pustulosis, a severe cutaneous drug reaction (Navarini *et al.*, 2013; Setta-Kaffetzi *et al.*, 2013). IL-36 is absent in normal skin but is induced by inflammatory cytokines such as tumor necrosis factor-α, IL-17A, and IL-22 (Carrier *et al.*, 2011). When functional IL-36RN is absent or underproduced, overexpressed IL-36 can induce neutrophil-rich infiltration. Tumor necrosis factor-α is often elevated in the blood of pregnant women, whereby it induces various serious diseases (Mallmann *et al.*, 1991). As for skin diseases, tumor necrosis factor-α sometimes causes exacerbation of PV lesions in pregnant women (Puig *et al.*, 2010). Hence, it is very likely that a pregnant woman who has the *IL36RN* mutation occasionally cannot produce enough IL-36RN to adequately antagonize IL-36 excessively induced by inflammatory cytokines, and this imbalance results in IH.

After longstanding controversy over whether IH is an independent disease

Abbreviations: GPP, generalized pustular psoriasis; IH, impetigo herpetiformis; IL-36RN, IL-36 receptor antagonist; PV, psoriasis vulgaris

Accepted article preview online 9 April 2014; published online 1 May 2014

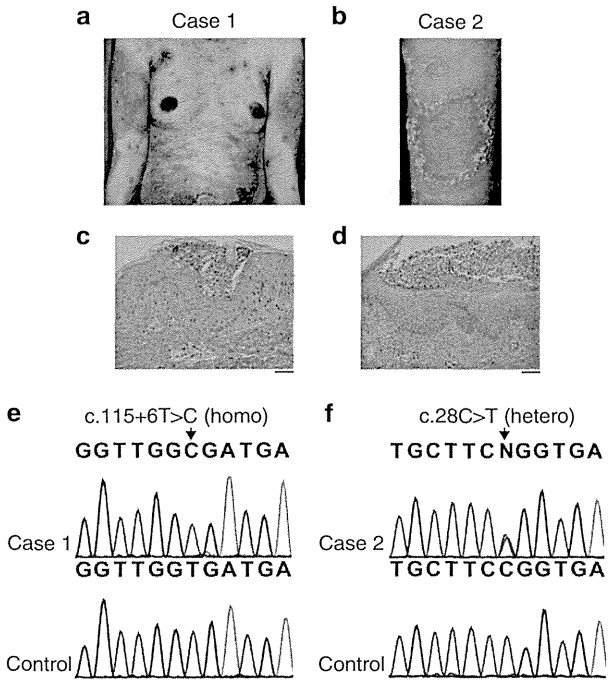

Figure 1. Clinical features, pathological findings of pustules, and mutation analysis of *IL36RN* in the patients. The clinical features of Cases 1 and 2 (**a**, **b**) are shown. Pustules on background erythema are seen on the trunk and arms. The pathology of the pustules is indicated for Cases 1 and 2 (**c**, **d**). Spongiosis of Kogoj and acanthosis are observed in the epidermis of the pustular erythematous lesions on the trunks. Scale bar = 50 μm for **c** and 100 μm for **d**. Direct sequencing reveals the homozygous mutation c.115 + 6T>C in Case 1 (**e**) and the heterozygous mutation c.28C>T in Case 2 (**f**).

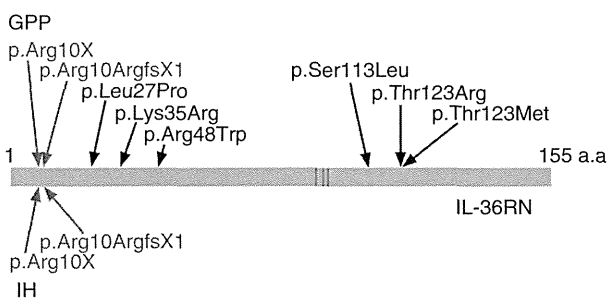

Figure 2. The second structure of IL-36RN and location of all *IL36RN* mutations ever reported in generalized pustular psoriasis (GPP) and impetigo herpetiformis (IH). All *IL36RN* mutations ever reported in GPP and IH (including in the present report) are shown (Kanazawa *et al.*, 2013). The blue characters indicate truncating mutations, and the black characters indicate missense mutations. Red lines show critical residues that mediate receptor interaction, such as Tyr89, Glu94, and Lys96 of IL36-RN (Sugiura *et al.*, 2013).

entity from GPP, today there is the consensus that IH is not a distinct entity but is identical to GPP, i.e., IH is GPP occurring during pregnancy (Lotem *et al.*, 1989; Robinson *et al.*, 2012). However, there have been no reports with experimental or genetic evidence to bolster the assertion that IH and GPP are identical diseases. This report clearly shows IH patients with homozygous or heterozygous *IL36RN* mutations. Case 1 was affected with IH only once in the gestational period. In this context, the present case suggests that IH and GPP, especially GPP alone, are identical diseases caused by *IL36RN* mutations. Future study should elucidate the proportion of IH cases that are *IL36RN* negative; however, given that the majority of GPP alone is associated with *IL36RN* mutations, we consider that mutation analysis of *IL36RN* is a very promising method for the prediction of IH risk to prevent subsequent serious complications in the patient and the fetus.

CONFLICT OF INTEREST

The authors state no conflict of interest.

ACKNOWLEDGMENTS

We thank Haruka Ozeki and Yuka Terashita for their technical help in analyzing *IL36RN* mutations. This study was supported in part by Grant-in-Aid for Scientific Research (C) 23591617 (to KS) and Grant-in-Aid for Scientific Research (A) 23249058 (to MA) from the Ministry of Education, Culture, Sports, Science and Technology of Japan.

Kazumitsu Sugiura[1], Naoki Oiso[2], Shin Iinuma[3], Hiromasa Matsuda[2], Masako Minami-Hori[3], Akemi Ishida-Yamamoto[3], Akira Kawada[2], Hajime Iizuka[3] and Masashi Akiyama[1]

[1]Department of Dermatology, Nagoya University Graduate School of Medicine, Nagoya, Japan; [2]Faculty of Medicine, Department of Dermatology, Kinki University, Osaka-Sayama, Japan and [3]Department of Dermatology, Asahikawa Medical University, Asahikawa, Japan
E-mail: kazusugi@med.nagoya-u.ac.jp or makiyama@med.nagoya-u.ac.jp

SUPPLEMENTARY MATERIAL

Supplementary material is linked to the online version of the paper at http://www.nature.com/jid

REFERENCES

Capon F (2013) IL36RN mutations in generalized pustular psoriasis: just the tip of the iceberg? *J Invest Dermatol* 133:2503–4

Carrier Y, Ma HL, Ramon HE *et al.* (2011) Inter-regulation of Th17 cytokines and the IL-36 cytokines *in vitro* and *in vivo*: implications in psoriasis pathogenesis. *J Invest Dermatol* 131:2428–37

Kanazawa N, Nakamura T, Mikita N *et al.* (2013) Novel IL36RN mutation in a Japanese case of early onset generalized pustular psoriasis. *J Dermatol* 40:749–51

Korber A, Mossner R, Renner R *et al.* (2013) Mutations in IL36RN in patients with generalized pustular psoriasis. *J Invest Dermatol* 133:2634–7

Li M, Han J, Lu Z *et al.* (2013) Prevalent and rare mutations in IL-36RN gene in Chinese patients with generalized pustular psoriasis

and psoriasis vulgaris. *J Invest Dermatol* 133:2637–9

Lotem M, Katzenelson V, Rotem A *et al.* (1989) Impetigo herpetiformis: a variant of pustular psoriasis or a separate entity? *J Am Acad Dermatol* 20:338–41

Mallmann P, Mallmann R, Krebs D (1991) Determination of tumor necrosis factor alpha (TNF alpha) and interleukin 2 (IL 2) in women with idiopathic recurrent miscarriage. *Arch Gynecol Obstet* 249:73–8

Navarini AA, Valeyrie-Allanore L, Setta-Kaffetzi N *et al.* (2013) Rare variations in IL36RN in severe adverse drug reactions manifesting as acute generalized exanthematous pustulosis. *J Invest Dermatol* 133:1904–7

Puig L, Barco D, Alomar A (2010) Treatment of psoriasis with anti-TNF drugs during pregnancy: case report and review of the literature. *Dermatology* 220:71–6

Robinson A, Van Voorhees AS, Hsu S *et al.* (2012) Treatment of pustular psoriasis: from the Medical Board of the National Psoriasis Foundation. *J Am Acad Dermatol* 67:279–88

Sauer GC, Geha BJ (1961) Impetigo herpetiformis. Report of a case treated with corticosteroid-review of the literature. *Arch Dermatol* 83:119–26

Setta-Kaffetzi N, Navarini AA, Patel VM *et al.* (2013) Rare pathogenic variants in IL36RN underlie a spectrum of psoriasis-associated pustular phenotypes. *J Invest Dermatol* 133:1366–9

Sugiura K, Muto M, Akiyama M (2014a) CARD14 c.526G>C (p.Asp176His) is a significant risk factor for generalized pustular psoriasis with psoriasis vulgaris in the Japanese cohort. *J Invest Dermatol.* (in press)

Sugiura K, Shoda Y, Akiyama M (2014b) Generalized pustular psoriasis triggered by amoxicillin in monozygotic twins with compound heterozygous IL36RN Mutations: comment on the article by Navarini *et al. J Invest Dermatol* 134:578–9

Sugiura K, Takemoto A, Yamaguchi M *et al.* (2013) The majority of generalized pustular psoriasis without psoriasis vulgaris is caused by deficiency of interleukin-36 receptor antagonist. *J Invest Dermatol* 133:2514–21

OPEN ACCESS Freely available online

PLOS | GENETICS

Revertant Mutation Releases Confined Lethal Mutation, Opening Pandora's Box: A Novel Genetic Pathogenesis

Yasushi Ogawa[1], Takuya Takeichi[1¤], Michihiro Kono[1], Nobuyuki Hamajima[2], Toshimichi Yamamoto[3], Kazumitsu Sugiura[1], Masashi Akiyama[1]*

1 Department of Dermatology, Nagoya University Graduate School of Medicine, Nagoya, Japan, **2** Department of Healthcare Administration, Nagoya University Graduate School of Medicine, Nagoya, Japan, **3** Department of Legal Medicine and Bioethics, Nagoya University Graduate School of Medicine, Nagoya, Japan

Abstract

When two mutations, one dominant pathogenic and the other "confining" nonsense, coexist in the same allele, theoretically, reversion of the latter may elicit a disease, like the opening of Pandora's box. However, cases of this hypothetical pathogenic mechanism have never been reported. We describe a lethal form of keratitis-ichthyosis-deafness (KID) syndrome caused by the reversion of the *GJB2* nonsense mutation p.Tyr136X that would otherwise have confined the effect of another dominant lethal mutation, p.Gly45Glu, in the same allele. The patient's mother had the identical misssense mutation which was confined by the nonsense mutation. The biological relationship between the parents and the child was confirmed by genotyping of 15 short tandem repeat loci. Haplotype analysis using 40 SNPs spanning the >39 kbp region surrounding the *GJB2* gene and an extended SNP microarray analysis spanning 83,483 SNPs throughout chromosome 13 in the family showed that an allelic recombination event involving the maternal allele carrying the mutations generated the pathogenic allele unique to the patient, although the possibility of coincidental accumulation of spontaneous point mutations cannot be completely excluded. Previous reports and our mutation screening support that p.Gly45Glu is in complete linkage disequilibrium with p.Tyr136X in the Japanese population. Estimated from statisitics in the literature, there may be approximately 11,000 p.Gly45Glu carriers in the Japanese population who have this second-site confining mutation, which acts as natural genetic protection from the lethal disease. The reversion-triggered onset of the disesase shown in this study is a previously unreported genetic pathogenesis based on Mendelian inheritance.

Citation: Ogawa Y, Takeichi T, Kono M, Hamajima N, Yamamoto T, et al. (2014) Revertant Mutation Releases Confined Lethal Mutation, Opening Pandora's Box: A Novel Genetic Pathogenesis. PLoS Genet 10(5): e1004276. doi:10.1371/journal.pgen.1004276

Editor: Nancy B. Spinner, University of Pennsylvania, United States of America

Received December 18, 2013; **Accepted** February 13, 2014; **Published** May 1, 2014

Funding: This study was supported in part by Grant-in-Aid for Scientific Research (A) 23249058 (MA) from the Ministry of Education, Culture, Sports, Science and Technology of Japan. (http://www.jsps.go.jp/english/e-grants/). The funders had no role in study design, data collection and analysis, decision to publish, or preparation of the manuscript.

Competing Interests: The authors have declared that no competing interests exist.

* E-mail: makiyama@med.nagoya-u.ac.jp

¤ Current address: St John's Institute of Dermatology, 9th Floor, Tower Wing, Guy's Hospital, London, United Kingdom

Introduction

A nonsense mutation may, in theory, disrupt and thus "confine" the effects of another dominant pathogenic mutation when the two mutations coexist in the same allele of a single gene. Furthermore, in such cases, reversion of the confining nonsense mutation may paradoxically elicit a congenital disease, although proven cases of this hypothetical pathogenesis have not been reported.

Keratitis-ichthyosis-deafness (KID) syndrome (OMIM 148210) is a rare congenital ectodermal disorder characterized by vascularizing keratitis, ichthyosiform erythroderma and sensorineural hearing loss [1]. KID syndrome is mainly caused by a heterozygous germ line missense mutation in GJB2 (Entrez Gene ID: 2706) encoding connexin 26 (Cx26) (RefSeq: NM_004004.5) [2–4].

Here we report a case of KID syndrome where the reversion of a missense mutation induced a lethal disease. We encountered a girl with KID syndrome from obviously healthy parents, and sequence analysis of *GJB2* revealed a heterozygous missense mutation, p.Gly45Glu, in the patient. Unexpectedly, her healthy mother also had the heterozygous missense mutation p.Gly45Glu, as well as another heterozygous nonsense mutation: p.Tyr136X. From these findings, we hypothesized that the p.Tyr136X mutation confines the pathogenic effect of p.Gly45Glu in the mother and that the reversion of p.Tyr136X triggered the onset of KID syndrome in the patient. In the present study, TA cloning and haplotype analysis of the family confirmed that an allelic recombination event involving the maternal allele carrying the two mutations generated the pathogenic allele unique to the patient. Furthermore, cotransfection experiments and a neurobiotin uptake assay clearly demonstrated that the p.Tyr136X mutation confines the pathogenic effects of the p.Gly45Glu mutation. Thus, to our knowledge, the present findings provide the first evidence of reversion-triggered onset of a congenital disease.

Results

The Patient's Mother Had Both *GJB2* Lethal Missense Mutation and Confining Nonsense Mutation, Although the Patient Had Only the Lethal One

The KID syndrome patient is a girl born from apparently healthy Japanese parents. She showed ichthyosiform erythroderma

Author Summary

Loss of gene functions due to nonsense mutations is a typical pathogenic mechanism of hereditary diseases. They may, however, in certain genetic contexts, confine the effects of other dominant pathogenic mutations and suppress disease manifestations. We report the first instance in the literature where the reversion of a "confining" nonsense mutation in *GJB2* gene released the dominant pathogenic effect of a coexsisting gain-of-function mutation, eliciting the lethal form of keratitis-ichthyosis-deafness syndrome (KID). We describe this form of KID syndrome caused by the reversion of the *GJB2* nonsense mutation p.Tyr136X that would otherwise have confined the effect of another dominant lethal mutation, p.Gly45Glu, in the same allele. The patient's mother had the identical misssense mutation which was confined by the nonsense mutation. An epidemiologic estimation demonstrates that approximately 11,000 individuals in the Japanese population may have the same lethal *GJB2* mutation, nonetheless protected from the manifestation of the syndrome because they also inherit the common "confining" nonsense mutation. The reversion-triggered onset of the disease shown in this study is a previously unreported genetic pathogenesis based on Mendelian inheritance.

at birth, and later she developed typical manifestations that lead to the diagnosis of KID syndrome (Figure 1A). Despite intensive care, she died of the disease.

Sequence analysis of *GJB2* was performed to confirm the diagnosis. Direct sequencing of PCR fragments spanning all the exons of *GJB2* revealed a heterozygous missense mutation, c.134G>A (p.Gly45Glu), in exon 2 of *GJB2* in the patient and her mother, but not in her father (Figure 1B). Her mother had an additional heterozygous nonsense mutation, c.408C>A (p.Tyr136X), in the same exon (Figure 1B). TA cloning analysis showed that the c.408C>A and c.134G>A mutations were in cis configuration. All family members uniformly harbored the two known non-pathological SNPs [5] c.79G>A (p.Val27Ile) (rs2274084) and c.341A>G (p.Glu114Gly) (rs2274083) heterozygously and in trans configuration with the c.134G>A or c.408C>A mutation (Figure 1C and 2A). The existence of the *GJB2* mRNA harboring the c.134G>A missense mutation in the patient's skin was verified by a RT-PCR assay (Figure S1). To confirm the biological relationship between the patient and her parents, we genotyped for 15 short tandem repeat (STR) loci with tetranucleotide repeat units using a multiplex kit. Since all of the genotypes for 15 STR loci were consistent with the relationship between the parents and child and each combined probability of exclusion and paternity was calculated as 0.999999997 and 0.9999999986, respectively, the authenticity of biological relationship between the parents and the child was confirmed accurately (Tables S1 and S2).

Revertant Mutation of Confining Nonsense Mutation Occurred in the Patient's Pathogenic Allele of *GJB2*

To elucidate the origin of the c.134G>A mutation in the patient, haplotype analysis was performed. Forty SNPs annotated by the International HapMap Project [6] spanning the >39 kbp region surrounding the *GJB2* gene were sequenced. Fourteen SNPs were found to be heterozygous in one or more of the family members (Figure 1C and S2). TA cloning analysis mapped the heterozygous SNPs into three separate genetic regions (Figure 1C). All family members had at least one common haplotype in each genetic region, suggesting that they share a haplotype in the > 39 kb genetic region we studied. Unexpectedly, the patient harbored a unique haplotype that was not seen in either of her parents (Figure 1C). No evidence of spontaneous mutations was found besides these SNP sites through the direct sequencing of the entire coding region of *GJB2*.

We performed an extended SNP microarray analysis spanning 83,483 SNPs throughout chromosome 13. No apparent chromosomal aberration was detected besides a 1,430 kbp copy-number neutral loss-of-heterozygosity region on 13q31.1 which was unique to the patient's genome.

From these findings, we reasoned that an allelic recombination event involving the shared allele (Figure 1C, shown in blue) and the maternally unique allele (Figure 1C, shown in orange) generated the haplotype unique to the patient (see also the Discussion section below), since it differs by three or more base pairs from the counterparts carried by either parent, giving only a remote possibility of coincidental accumulation of spontaneous point mutations at these specific SNP sites. The latter possibility, however, cannot be completely excluded.

The blood cells of the patient did not show mosaicism, and the patient's skin symptoms were fairly evenly distributed over the entire body surface. These findings suggest that the patient was not mosaic for the *GJB2* mutation. Thus, we consider the reversion leading to the pathogenic allele in the patient to be a pre-zygotic event.

Gap Junctions Containing p.Gly45Glu-Mutant Connexin 26 (CX26) Showed Aberrant Gating Activity, Whereas p.Gly45Glu/p.Tyr136X-Mutant CX26 Were Excluded from Functional Gap Junction Formation

As described above, the patient who harbored the p.Gly45Glu mutation manifested the disease, while the mother who harbored the mutations p.Gly45Glu and p.Tyr136X was apparently unaffected (Figure 2A). A heterozygous *de novo* p.Gly45Glu mutation is known to cause the lethal form of KID syndrome [3], and its molecular pathogenic mechanism has been well described [7–9]. Cx26, the product of *GJB2*, is a gap junction protein with four transmembrane domains and two extracellular domains (Figure 2B). The Cx26 molecule is a protomer of a hexameric connexon, and two connexons expressed on the membranes of neighboring cells connect to form a gap junction channel [10]. Gly45 locates at a domain that lines the channel pore and probably mediates voltage sensing [10]. Connexons containing p.Gly45Glu mutants function as hemichannels with aberrantly increased activity [7,8] that leads to the disease manifestations [3,9]. It is also known that, besides KID syndrome, biallelic loss of function of *GJB2* causes autosomal recessive non-syndromic hearing loss (NSHL) [11]. The fact that the p.Gly45Glu/p.Tyr136X mutation homozygously or compound heterozygously causes NSHL suggests that this mutation leads to total loss of function for the *GJB2* product [5].

These considerations lead us to hypothesize that the p.Tyr136X mutation confines and rescues the dominant pathogenic effect of the p.Gly45Glu mutation. Since inter-protomer interactions of Cx26 require the fourth transmembrane domain [10] that is terminated by the p.Tyr136X mutation (Figure 2 A and B), a Cx26 carrying p.Gly45Glu/p.Tyr136X alteration would be excluded from the hexameric connexons.

This phenomenon, in which a second-site mutation cancels an exsisting pathogenic mutation, was previously reported; it is called "partial reversion", because the wild-type allele itself is not

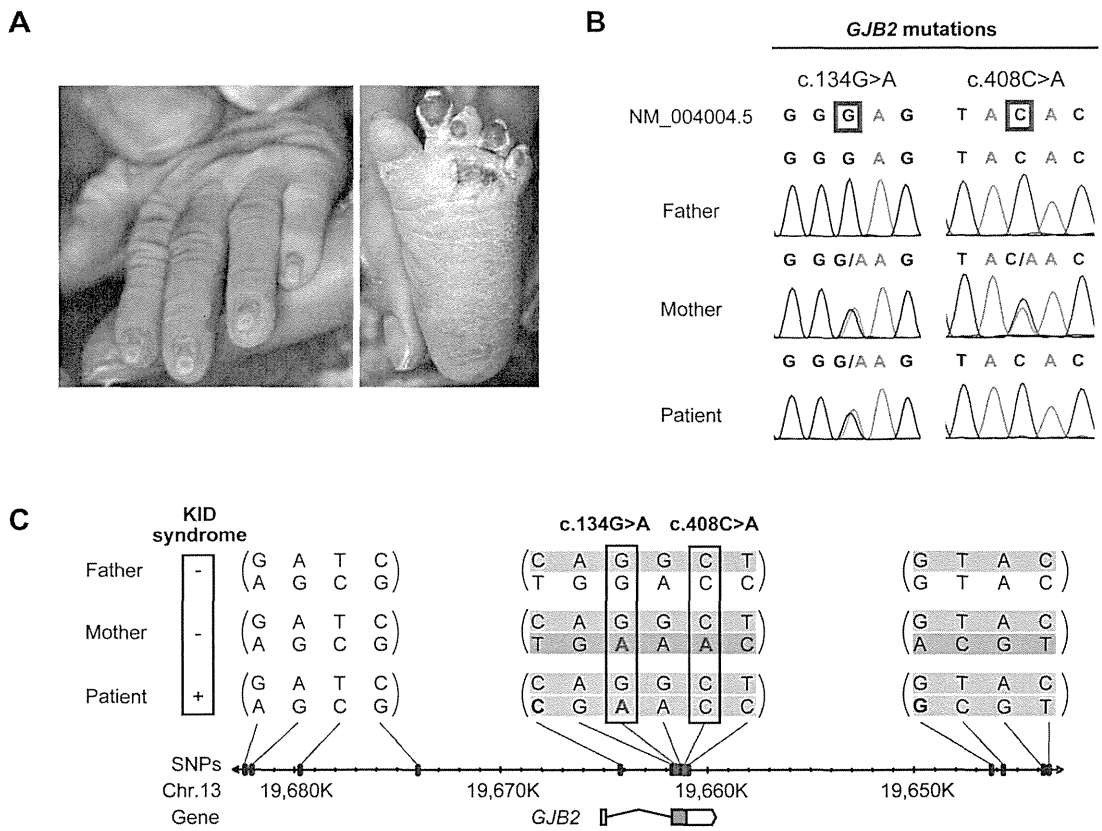

Figure 1. Sequence and haplotype analysis of the present case of KID syndrome. (A) Clinical manifestations of the patient are shown. Marked hyperkeratosis of the palms and soles is seen. (B) Identification of c.134G>A and c.408C>A mutations in the patient and her parents. The patient is compound heterozygous for the two mutations. (C) Haplotype analysis of the family members. Fourteen heterozygous SNPs spanning > 39 kbp surrounding the *GJB2* gene are identified and assembled into three contigs (shown in parenthesis). The nucleotides altered by the c.134G>A and c.408C>A mutations are boxed. The altered nucleotides are in red. The patient and her parents share a single haplotype (top; blue background). The patient has a unique haplotype (bottom; yellow background) that is not harbored by either parent. The maternally unique haplotype is shown in orange.

doi:10.1371/journal.pgen.1004276.g001

attained, although the seoncd-site mutation rescues the disease [12].

To test this hypothesis, we observed the colocalization of fluorescent-tagged Cx26 variants in HeLa cells. The father had wild-type and p.Val27Ile/p.Glu114Gly variant alleles (Figure 2A). When these Cx26s were cotransfected, they together formed gap junctions, suggesting that both proteins retain their native functions (Figure 3A). The Cx26 p.Gly45Glu/p.Tyr136X mutant failed to enter the gap junction generated by Cx26 p.Val27Ile/p.Glu114Gly, demonstrating that only the latter form comprises the functional gap junctions in the mother (Figure 3A). Cx26 p.Gly45Glu colocalized with the p.Val27Ile/p.Glu114Gly variant but failed to form gap junctions (Figure 3A). In a neurobiotin uptake assay, which monitors channel activity as cellular uptake of a neurobiotin tracer [9], only the p.Gly45Glu mutant and not the p.Gly45Glu/p.Tyr136X mutant induced the aberrant uptake (Figure 3B).

Discussion

Many cases of revertant mosaicism have been reported as "natural gene therapy" where the mitotic recombination results in revertant mutations that mitigate the disease symptoms [13–16]. However, the present study is the first report to demonstrate a mutant reversion triggering a genetic disease.

The present data of genomic DNA sequencing and haplotype analysis demonstrate that the patient and her father share an identical haplotype (Figure 1C, shown in blue). We hypothesized that the entire blue allele in the patient's genome was derived from the father, while the other allele (Figure 1C, shown in yellow) was basically derived from the mother. It seemed, however, that this allele underwent pre-zygotic reversion during meiosis of the maternal gamete. The fact that the patient's unique allele (Figure 1C, shown in yellow) differs by three non-continuous SNPs from the unique maternal allele (Figure 1C, shown in orange) while the neighboring SNPs are conserved might be explained by multiple events of gene conversion involving both of the maternal alleles (Figure 1C, shown in blue and orange) that may have occurred in this genetic region.

Double cross-over also might account for the recombination, but it is less likely, considering that the non-conserved and conserved SNPs in the patient's allele reside within close proximity (Figure 1C); the average length of the gene conversion tract is estimated to be in the range of 55–290 bp, whereas the cross-over tracts are typically longer [17].

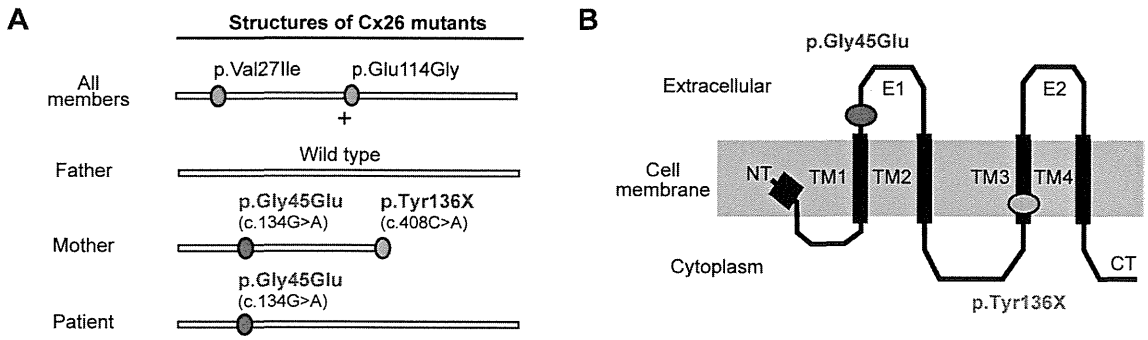

Figure 2. Configurations and topological mapping of the *GJB2* mutations in the family. (A) Structures of Cx26 mutants. The mutations/variants found in each allele of the family members are shown. p.Val27Ile and p.Glu114Gly are non-pathological variants. (B) Topological mapping of the Cx26 mutations. p.Gly45Glu (red) is located in the first extracellular loop domain and is thought to affect the channel activity of gap junctions. TM1–4: transmembrane domain 1–4; E1–2: extracellular domain 1–2; NT: N terminus; CT: C terminus.
doi:10.1371/journal.pgen.1004276.g002

Mitotic gene conversion has been found in some cases of revertant mosaicism in cutaneous disease, including generalized atrophic benign epidermolysis bullosa [12,13]. We are unaware of any previous report of multiple gene conversions within a relatively short genetic segment as in the present case. However, the present data compel us to consider that it occurred. Since the patient's unique allele differs by three or more base pairs from the counterparts carried by either parent, we judge the possibility of coincidental accumulation of spontaneous point mutations at these specific SNP sites to be highly unlikely. This possibility, however, cannot be completely excluded.

As evidence supporting our hypothesis, consistent with a previous report [9], we clearly demonstrated that Cx26 p.Gly45Glu colocalized with the p.Val27Ile/p.Glu114Gly variant but failed to form gap junctions (Figure 3A). Previous studies have shown that Cx26 p.Gly45Glu forms hemichannels that are aberrantly activated at low extracellular Ca2+ levels [9]. The present study used a neurobiotin uptake assay [9] to show that only the p.Gly45Glu mutant and not the p.Gly45Glu/p.Tyr136X mutant induces the aberrant uptake (Figure 3B). These results taken together support the model in which the p.Tyr136X mutation confines the dominant gain-of-function effect of the p.Gly45Glu mutation to prevent the onset of the disease (Figure 4). Such secondary effects of revertants may pose a challenge in genetic analyses of extended genes or more than one gene with functional interactions.

Interestingly, in the group of Japanese patients with bilateral sensorineural hearing loss, it is not uncommon to find *GJB2* p.Gly45Glu carriers, but none of them are affected by KID syndrome [5]. They uniformly have a tandem p.Tyr136X mutation, as in the mother of the present case [5]. Thus, we hypothesized that, in the Japanese population, carriers of p.Gly45Glu are protected from the lethal form of KID syndrome by the tandem, confining mutation p.Tyr136X.

To clarify the frequency of the p.Gly45Glu mutation in the entire Japanese population, we performed screening analysis for the two mutations p.Gly45Glu and p.Tyr136X in a normal control group consisting of 920 overall healthy Japanese individuals (1,840 alleles). Neither p.Gly45Glu nor p.Tyr136X was found in any of the 1,840 alleles (data not shown). Tsukada *et al.* [5] also reported that neither p.Gly45Glu nor p.Tyr136X was found in 252 Japanese healthy control individuals (504 control Japanese alleles). These results indicate that the alleles with tandem p.Gly45Glu and p.Tyr136X mutations are infrequent in the general Japanese population. However, in the epidemiological statistics of Tsukada *et al.* [5], we found screening data for *GJB2* mutations in Japanese patients with sensorineural hearing loss. The report revealed that, among 1,343 Japanese patients with hearing loss, 33 patients had one or two p.Gly45Glu alleles (34 p.Gly45Glu alleles in 2686 alleles for an allele frequency of 1.27%; 33 carriers in 1,343 patients for a carrier rate of 2.46%). This means 2.46% of Japanese patients with bilateral sensorineural hearing loss have one or two p.Gly45Glu alleles. As for the prevalence of sensorineural hearing loss, it was reported that 3.5 per 1,000 individuals in the entire population have bilateral sensorineural hearing loss [18]. Thus, calculating from these epidemiological statistics, we estimate that 8.6 per 100,000 individuals, or approximately 11,000 individuals in the entire Japanese population, have one or two p.Gly45Glu alleles. However, no patient with the lethal form of KID syndrome due to p.Gly45Glu has been reported in the Japanese population as far as we know, although the mutation p.Gly45Glu has been reported as a cause of the lethal form of KID syndrome in several European patients [3,19–22].

Tsukada *et al.* [5] reported that all 34 alleles with p.Gly45Glu found in the Japanese patients with sensorineural hearing loss also had p.Tyr136X, suggesting that p.Gly45Glu is in complete linkage disequillibrium with p.Tyr136X in the Japanese population. In our mutation screening, no allele carrying either or both mutations, p.Gly45Glu and p.Tyr136X, was found in 920 Japanese individuals (1,840 alleles) and these results support the idea that p.Gly45Glu is in complete LD with p.Tyr136X in the Japanese population.

In light of this, we conclude that, even though individuals may have the dominant lethal mutation p.Gly45Glu, the confining mutation p.Tyr136X *in cis* configuration protects against the disease, KID syndrome, in the approximately 11,000 Japanese individuals in the entire Japanese population who harbor p.Gly45Glu. The allele with the tandem mutations p.Gly45Glu and p.Tyr136X causes hearing loss in an autosomal recessive manner. Most carriers of the tandem mutations in the Japanese population are heterozygous for the allele, such as the patient's mother in the present study, and are not affected with hearling loss.

In summary, our findings demonstrate that the second-site confining mutation is an imporatant genetic protection mechanism, and its loss, like the opening of Pandora's box, is a novel genetic pathogenesis that releases the hidden genetic disease.

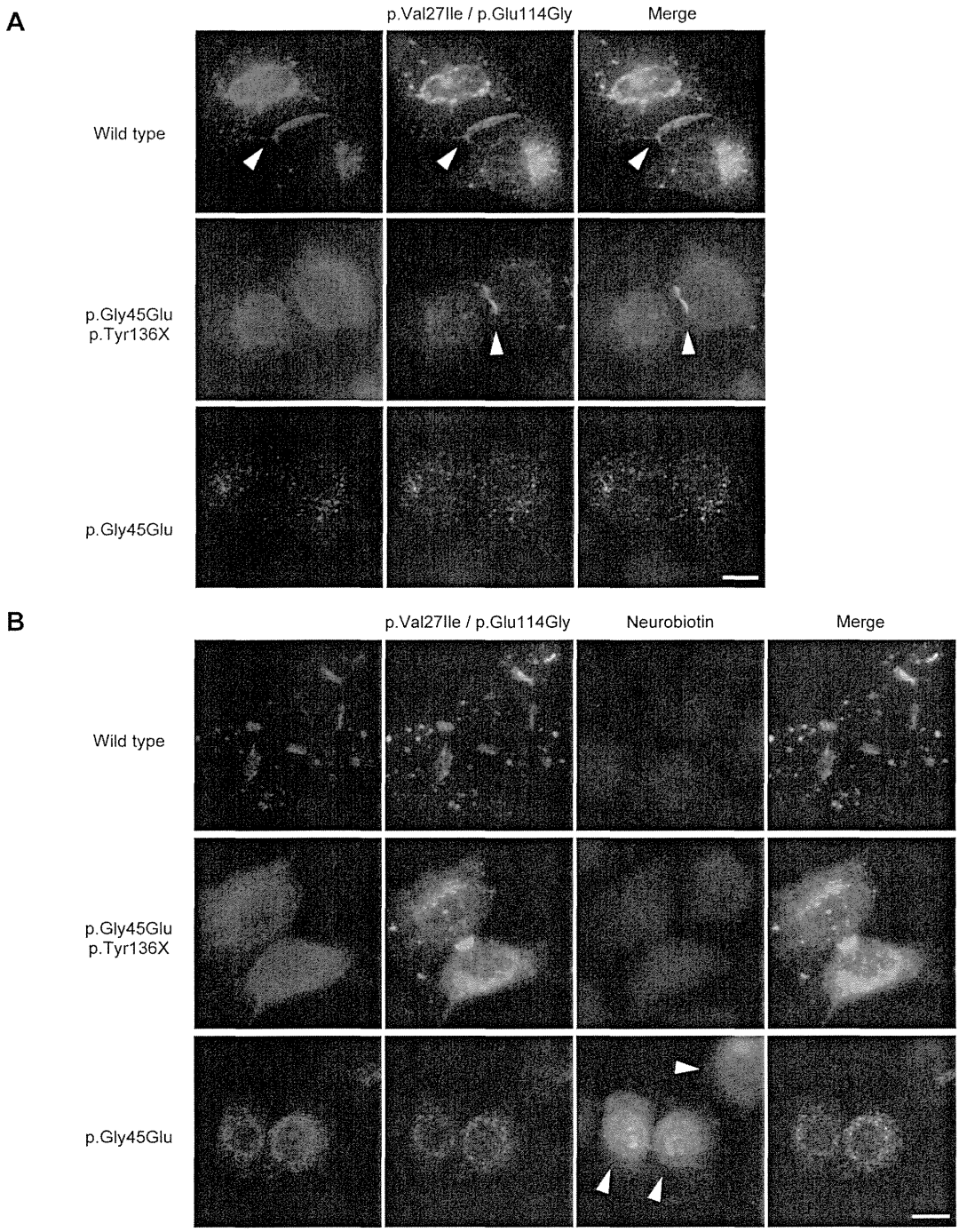

Figure 3. The p.Tyr136X mutation confines the effect of the pGly45Glu mutation. (A) Gap junction formation by the transfected Cx26 variants. Each panel contains two co-transfected cells connected to each other. Wild-type, p.Gly45Glu/p.Tyr136X and p.Gly45Glu mutants of Cx26 were tagged with monomeric Red Fluorescent Protein (mRFP) and co-transfected with Green Fluorescent Protein (EGFP)-tagged Cx26 p.Val27Ile/p.Glu114Gly into HeLa cells as indicated. Gap junction formation sites are indicated by arrowheads. The combination of WT Cx26 and Cx26 p.Val27Ile/p.Glu114Gly (top row) results in gap junctions that consist of both Cx26 proteins (yellow signal). The combination of Cx26 p.Gly45Glu/p.Tyr136X and Cx26 p.Val27Ile/p.Glu114Gly (middle row) results in gap junctions with only Cx26 p.Val27Ile/p.Glu114Gly (green signal). No apparent gap junction formation is seen when Cx26 p.Gly45Glu and Cx26 p.Val27Ile/p.Glu114Gly are cotransfected (bottom row). (B) Aberrant gate opening detected with neurobiotin uptake assay. Fluorescent-tagged Cx26s were cotransfected into HeLa cells as indicated, and treated with neurobiotin in a calcium-free condition. Uptake was detected with AlexaFluor350 streptoavidin dye (blue). Aberrant uptake of neurobiotin is observed only in cells cotransfected with Cx26 p.Gly45Glu and Cx26 p.Val27Ile/p.Glu114Gly (bottom row).
doi:10.1371/journal.pgen.1004276.g003

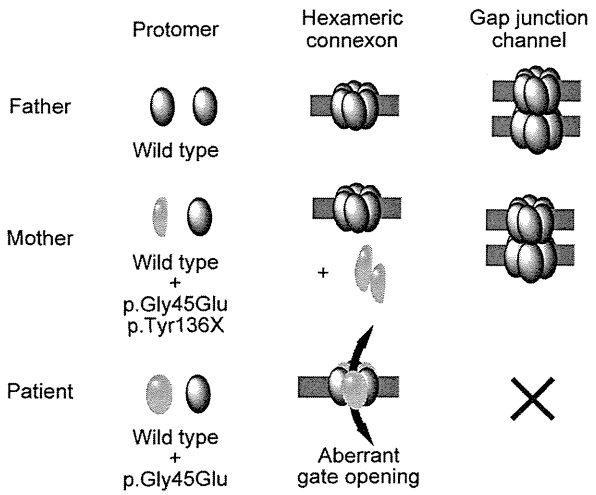

Figure 4. Schematic of the mechanism whereby the p.Tyr136X mutation confines the effect of the p.Gly45Glu mutation. The truncated Cx26 peptides produced from the mutant p.Gly45Glu/p.Tyr136X are not incorporated into connexons or gap junctions (middle row), although Cx26 peptides derived from the mutant p.Gly45Glu are incorporated into connexons, resulting in aberrant gate opening and malformation of gap junctions (bottom row).
doi:10.1371/journal.pgen.1004276.g004

Materials and Methods

Ethics Statement

This study was approved by the Bioethics Committee of the Nagoya University Graduate School of Medicine and was conducted according to The Declaration of Helsinki Principles. Written informed consent was obtained from the parents.

The Patient and Her Parents

The patient was referred and seen at the Outpatient Clinic of Dermatology, Nagoya University Hospital.

Sequence Analysis and TA Cloning

Genomic DNA extracted from peripheral blood was used as a template for PCR amplification, followed by direct automated sequencing. The entire coding regions of *GJB2* including the exon/intron boundaries were sequenced as reported elsewhere [4]. TOPO-TA cloning kit (Life Technologies) was used for TA cloning analyses. PCR primers were designed to amplify the genetic regions containing the selected SNPs, and the acquired PCR products were analyzed by direct sequencing. For amplification of PCR fragments longer than 1,000 base pairs, KOD-Plus-Neo polymerase (Toyobo) or PrimeScript GXL polymerase (Takara Bio) was used and the PCR products were cloned with the TOPO XL-TA Cloning Kit (Life Technologies) after the addition of a 3′-adenine overhang.

Verification of the Parent-Child Relationship

The parent-child relationship was validated using AmpFlSTR Identifier plus PCR amplification kit (Applied Biosystems) according to the manufacturer's instructions. The combined probability of exclusion and the combined probability of paternity (in the case of the odds ratio for prior probability = 1) for 15 STR loci were calculated to confirm the authenticity of the biological relationship between the parents and the child.

Genotyping of *GJB2* Mutations in 920 Japanese Control Individuals

Genomic DNA was extracted from whole blood using the QIAamp DNA Blood Maxi Kit (Qiagen). Real-time PCR-based genotyping of the *GJB2* mutations was performed with TaqMan MGB probe genotyping assay according to the manufacturer's instructions provided by Roche Diagnostics. To detect an allele of each mutation, a set of two TaqMan MGB probes labeled with a fluorescent dye (FAM or VIC) and a quencher dye (non-fluorescent dye; NFD) followed by minor groove binder (MGB), and sequence-specific forward and reverse primers were synthesized by Life Technologies Corporation. The sequences of assay probes/primers are shown in Table S3 in this article's supplementary material. Real-time PCR was performed with LightCycler 480 system II 384 plate (Roche Diagnostics) in a final volume of 5 µl containing 2× LightCycler 480 Probes Master (Roche Diagnostics), 200 nM probes for wild type and mutant each and 900 nM forward and reverse primers each, with 5 ng genomic DNA as the template. The thermal conditions were the following: 95°C for 10 min, followed by 45 cycles of 95°C for 10 s, 60°C for 60 s and 72°C for 1 s, with a final cooling at 40°C for 30 s. Endpoint fluorescence was measured for each sample well. Afterward, genotyping was performed using endpoint genotyping analysis in LightCycler 480 software.

Eight hundred and twenty controls were analyzed with the real-time PCR-based genotyping of *GJB2* mutations, and another 100 controls were analyzed with the direct automated sequencing for the entire coding region of *GJB2*.

GJB2 Expression Study

Total RNA from the formaldehyde-fixed paraffin-embedded skin sample of the patient was extracted using the RNeasy FFPE kit (Qiagen) and Deparaffinization Solution (Qiagen) according to the manufacturer's instructions. The total RNA was reverse-transcribed with a *GJB2* specific primer, 5′-GGATGTGGGAGATGGGGAAGTAGTG-3′, using PrimeScriptII 1st strand cDNA synthesis kit (Takara, Japan). The PCR fragment harboring c.134G>A mutation was amplified with primer sets, 5′-GGAAAGATCTGGCTCACCGTCCTC-3′ and 5′-CGTAGCACACGTTCTTGCAGCCTG-3′, and directly sequenced with the same primers.

SNP Array

Chromosome-wide genotyping was performed using HumanOmni2.5–8 BeadChip (Illumina), which covers a total of 2,379,855 SNPs throughout the genome, including 83,482 SNPs on chromosome 13. Genomic DNA was hybridized according to the manufacturer's instructions and data analysis was carried out using GenomeStudio software (Illumina).

Cell Culture

HeLa cells were cultured in Dulbecco's modified Eagle's medium (DMEM) containing 10% fetal calf serum. For transfection of plasmids, cells were seeded onto 8-well LabTek chamber slides (Thermo Scientific) and transfected with FuGene HD Transfection Reagent (Roche Applied Science) according to the manufacturer's instructions.

Plasmid Construction

The coding sequences of Cx26 variants were amplified from the genome of the patient or the parents, fused to cDNAs coding enhanced green fluorescent protein (EGFP) (Clontech) or monomeric red fluorescent protein (Clontech), and subcloned into

pcDNA3.1(-) plasmid using the InFusion HD Cloning Kit (Takara Bio). The coding sequences of the generated vectors were checked for PCR errors by direct sequencing.

Colocalization Assay

HeLa cells were cotransfected with the EGFP-tagged and mRFP-tagged vectors. Forty-eight hours after transfection, the cells were fixed with 4% formaldehyde. Fluorescent images were obtained using FSX-100 microscope system (Olympus).

Neurobiotin Uptake Assay

HeLa cells were cotransfected with EGFP-tagged and mRFP-tagged Cx26 variant expressing vectors, and neurobiotin uptake assay was performed as described elsewhere [9]. Briefly, cells were washed with calcium free Hank's buffered salt solution for 20 minutes and incubated with phosphate-buffered saline (PBS) containing 0.1 mg/ml neurobiotin (Vector Laboratories) for another 20 minutes. Cells were washed three times with PBS supplemented with 2 mM $CaCl_2$ for 10 minutes at 37°C. The cells were fixed with 4% formaldehyde and permeabilized and blocked with 3% BSA/0.1% Triton X-100/PBS for 1 hour. Then the cells are stained with 3% BSA/0.1% Triton X-100/PBS containing 10 μg/ml Alexa Fluor 350-streptoavidin (Life Technologies) for 1 hour, followed by three washes with 0.1% Triton X-100/PBS. Stained cells were fixed with ProLong Gold antifade reagent (Life Technologies) and fluorescent images were obtained.

Supporting Information

Figure S1 The *GJB2* mRNA harboring the missense mutation is expressed in the patient's skin. (A) RT-PCR from the total RNA extracted from a formaldehyde-fixed paraffin-embedded skin sample of the patient. A 136-bp PCR fragment was amplified from the *GJB2* cDNA obtained from the skin sample of the patient. (B) Detection of *GJB2* cDNA harboring the c.134G>A missense mutation. The PCR fragment was directly sequenced to confirm the expression of the mutant *GJB2* mRNA.
(TIF)

Figure S2 Summary of 40 SNPs spanning the >39 kbp region including GJB2. The SNPs inside the red box reside within the GJB2 gene. Note that the nucleotides are in the strand opposite those shown in Figure 1.
(TIF)

Table S1 Genotyping of the patient and her parents for 15 short tandem repeat (STR) loci.
(DOCX)

Table S2 The combined probability of exclusion and the combined probability of paternity.
(DOCX)

Table S3 The sequence of probes/primers for real-time PCR-based genotyping of *GJB2* mutations.
(DOCX)

Acknowledgments

We thank Professor Akimichi Morita and Dr. Emi Nishida for clinical information. We also thank Dr. Atsushi Enomoto and Kaori Ushida for technical assistance.

Author Contributions

Conceived and designed the experiments: YO KS MA. Performed the experiments: YO TT MK TY. Analyzed the data: YO KS TT MK TY MA. Contributed reagents/materials/analysis tools: NH. Wrote the paper: YO MK.

References

1. Skinner BA, Greist MC, Norins AL (1981) The keratitis, ichthyosis, and deafness (KID) syndrome. Arch Dermatol 117: 285–289.
2. Richard G, Rouan F, Willoughby CE, Brown N, Chung P, et al. (2002) Missense mutations in GJB2 encoding connexin-26 cause the ectodermal dysplasia keratitis-ichthyosis-deafness syndrome. Am J Hum Genet 70: 1341–1348.
3. Janecke AR, Hennies HC, Gunther B, Gansl G, Smolle J, et al. (2005) GJB2 mutations in keratitis-ichthyosis-deafness syndrome including its fatal form. Am J Med Genet A 133A: 128–131.
4. Arita K, Akiyama M, Aizawa T, Umetsu Y, Segawa I, et al. (2006) A novel N14Y mutation in Connexin26 in keratitis-ichthyosis-deafness syndrome: analyses of altered gap junctional communication and molecular structure of N terminus of mutated Connexin26. Am J Pathol 169: 416–423.
5. Tsukada K, Nishio S, Usami S (2010) A large cohort study of GJB2 mutations in Japanese hearing loss patients. Clin Genet 78: 464–470.
6. The International HapMap Consortium (2003) The International HapMap Project. Nature 426: 789–796.
7. Stong BC, Chang Q, Ahmad S, Lin X (2006) A novel mechanism for connexin 26 mutation linked deafness: cell death caused by leaky gap junction hemichannels. Laryngoscope 116: 2205–2210.
8. Gerido DA, DeRosa AM, Richard G, White TW (2007) Aberrant hemichannel properties of Cx26 mutations causing skin disease and deafness. Am J Physiol Cell Physiol 293: C337–345.
9. Mese G, Sellitto C, Li L, Wang HZ, Valiunas V, et al. (2011) The Cx26-G45E mutation displays increased hemichannel activity in a mouse model of the lethal form of keratitis-ichthyosis-deafness syndrome. Mol Biol Cell 22: 4776–4786.
10. Maeda S, Nakagawa S, Suga M, Yamashita E, Oshima A, et al. (2009) Structure of the connexin 26 gap junction channel at 3.5 A resolution. Nature 458: 597–602.
11. Kalatzis V, Petit C (1998) The fundamental and medical impacts of recent progress in research on hereditary hearing loss. Hum Mol Genet 7: 1589–1597.
12. Jonkman MF (1999) Revertant mosaicism in human genetic disorders. Am J Med Genet 85: 361–364.
13. Jonkman MF, Scheffer H, Stulp R, Pas HH, Nijenhuis M, et al. (1997) Revertant mosaicism in epidermolysis bullosa caused by mitotic gene conversion. Cell 88: 543–551.
14. Jonkman MF, Castellanos Nuijts M, van Essen AJ (2003) Natural repair mechanisms in correcting pathogenic mutations in inherited skin disorders. Clin Exp Dermatol 28: 625–631.
15. Choate KA, Lu Y, Zhou J, Choi M, Elias PM, et al. (2010) Mitotic recombination in patients with ichthyosis causes reversion of dominant mutations in KRT10. Science 330: 94–97.
16. Kiritsi D, He Y, Pasmooij AM, Onder M, Happle R, et al. (2012) Revertant mosaicism in a human skin fragility disorder results from slipped mispairing and mitotic recombination. J Clin Invest 122: 1742–1746.
17. Jeffreys AJ, May CA (2004) Intense and highly localized gene conversion activity in human meiotic crossover hot spots. Nat Genet 36: 151–156.
18. Morton CC, Nance WE (2006) Newborn hearing screening–a silent revolution. N Engl J Med 354: 2151–2164.
19. Griffith AJ, Yang Y, Pryor SP, Park HJ, Jabs EW, et al. (2006) Cochleosaccular dysplasia associated with a connexin 26 mutation in keratitis-ichthyosis-deafness syndrome. Laryngoscope 116: 1404–1408.
20. Jonard L, Feldmann D, Parsy C, Freitag S, Sinico M, et al. (2008) A familial case of Keratitis-Ichthyosis-Deafness (KID) syndrome with the GJB2 mutation G45E. Eur J Med Genet 51: 35–43.
21. Sbidian E, Feldmann D, Bengoa J, Fraitag S, Abadie V, et al. (2010) Germline mosaicism in keratitis-ichthyosis-deafness syndrome: pre-natal diagnosis in a familial lethal form. Clin Genet 77: 587–592.
22. Koppelhus U, Tranebjaerg L, Esberg G, Ramsing M, Lodahl M, et al. (2011) A novel mutation in the connexin 26 gene (GJB2) in a child with clinical and histological features of keratitis-ichthyosis-deafness (KID) syndrome. Clin Exp Dermatol 36: 142–148.

Allergy EUROPEAN JOURNAL OF ALLERGY AND CLINICAL IMMUNOLOGY

EAACI

Allergy

BRIEF COMMUNICATION

Comprehensive screening for a complete set of Japanese-population-specific filaggrin gene mutations

M. Kono[1], T. Nomura[2], Y. Ohguchi[2], O. Mizuno[2], S. Suzuki[2], H. Tsujiuchi[1], N. Hamajima[3], W. H. I. McLean[4], H. Shimizu[2] & M. Akiyama[1]

[1]Department of Dermatology, Nagoya University Graduate School of Medicine, Nagoya; [2]Department of Dermatology, Hokkaido University Graduate School of Medicine, Sapporo; [3]Department of Healthcare Administration, Nagoya University Graduate School of Medicine, Nagoya, Japan; [4]Centre for Dermatology and Genetic Medicine, Colleges of Life Sciences, Medicine, Dentistry & Nursing, University of Dundee, Dundee, UK

To cite this article: Kono M, Nomura T, Ohguchi Y, Mizuno O, Suzuki S, Tsujiuchi H, Hamajima N, McLean WHI, Shimizu H, Akiyama M. Comprehensive screening for a complete set of Japanese-population-specific filaggrin gene mutations. *Allergy* 2014; **69**: 537–540.

Keywords
allergic rhinitis; filaggrin; hay fever; mutation; real-time PCR.

Correspondence
Masashi Akiyama, Department of Dermatology, Nagoya University Graduate School of Medicine, 65 Tsurumai-cho, Showa-ku, Nagoya 466-8550, Japan.
Tel.: 81-52-744-2314
Fax: 81-52-744-2318
E-mail: makiyama@med.nagoya-u.ac.jp

Accepted for publication 27 December 2013

DOI:10.1111/all.12369

Edited by: Stephan Weidinger

Abstract

Mutations in *FLG* coding profilaggrin cause ichthyosis vulgaris and are an important predisposing factor for atopic dermatitis. Until now, most case–control studies and population-based screenings have been performed only for prevalent mutations. In this study, we established a high-throughput *FLG* mutation detection system by real-time PCR with a set of two double-dye probes and conducted comprehensive screening for almost all of the Japanese-population-specific *FLG* mutations (ten *FLG* mutations). The present comprehensive screening for all ten *FLG* mutations provided a more precise prevalence rate for *FLG* mutations (11.1%, $n = 820$), which seemed high compared with data of previous reports based on screening for limited numbers of *FLG* mutations. Our comprehensive screening suggested that population-specific *FLG* mutations may be a significant predisposing factor for hay fever (odds ratio = 2.01 [95% CI: 1.027–3.936, $P < 0.05$]), although the sample sizes of this study were too small for reliable subphenotype analysis on the association between *FLG* mutations and hay fever in the eczema patients and the noneczema individuals, and it is not clear whether the association between *FLG* mutations and hay fever is due to the close association between *FLG* mutations and hay fever patients with eczema.

Mutations in *FLG*, the gene-coding profilaggrin/filaggrin, are an important predisposing factor for atopic dermatitis (AD) (1) and are significantly associated with asthma with AD, mainly in the European population (2–4). The prevalence of *FLG* mutations in AD patients seems to be increasing (5).

The presence of population-specific FLG mutations has been reported in both Europeans and Asians (1, 6, 7) and is a serious obstacle to *FLG* mutation screening in each population. We established a real-time polymerase chain reaction (PCR)-based rapid detection system for Japanese-population-specific *FLG* mutations and performed high-throughput *FLG* screening on 820 residents in a rural area of Japan.

Subjects and methods

The subjects were 820 residents (284 males and 536 females) aged 39–90 years in Yakumo, a rural town in Hokkaido, Japan (8) (Data S1 and Table S1). The participants were requested to answer a questionnaire on health and daily lifestyle at the occasion of the health checkup. Patients with hay fever were defined as individuals reported to have had frequent episodes of all three symptoms of watery eyes, running nose, and sneezing. Patients with asthma were defined as individuals reported to have had a history of asthma, which was diagnosed by physicians. This study was approved by the Ethics Review Committee of Nagoya University Graduate School of Medicine. Ten *FLG* mutations have been identified in the Japanese population, nine of them found by our group (7). We have already performed the sequencing of all the coding regions of *FLG* for more than 30 Japanese families with ichthyosis vulgaris, to identify Japanese-specific *FLG* mutations comprehensively. We expect that screening for these ten mutations can detect almost all Japanese *FLG* mutation carriers. Thus, the present *FLG* mutation screening addressed those ten *FLG* mutations (Table 1). Real-time PCR-based genotyping

Table 1 *FLG* genotypes in the present cross-sectional study

Genotype	p.Arg501X	c.3321delA	p.Ser1695X	p.Gln1701X	p.Ser2554X	p.Ser2889X	p.Ser3296X	p.Lys4022X	p.Q1790X	c.441-442delAG	Combined
AA	820 (1.000)	810 (0.988)	820 (1.000)	818 (0.998)	806 (0.983)	785 (0.957)	816 (0.995)	796 (0.971)	816 (0.995)	820 (1.000)	729
Aa	0 (0)	10 (0.012)	0 (0)	2 (0.002)	14 (0.017)	35 (0.043)	4 (0.005)	24 (0.029)	4 (0.005)	0 (0)	89
aa	0	0	0	0	0	0	0	0	0	0	2*
Total	820	820	820	820	820	820	820	820	820	820	820
Allele freq.(a) (%)	0.0	0.61	0.0	0.12	0.85	2.13	0.24	1.46	0.24	0.0	5.65
HWE† test (chi-square test, *P*-value)	n.a.	0.861	n.a.	0.972	0.805	0.532	0.944	0.671	0.944	n.a.	n.a.

In genotype data columns, numbers are actual measurement data and actual genotype rate in parentheses.
*These data mean compound heterozygote.
†Hardy–Weinberg equilibrium.

of the *FLG* mutations was performed with TaqMan probe genotyping assay (Data S1 and Table S1).

Results and discussion

Of the 820 participants, 89 individuals were heterozygous for one of the ten *FLG* mutations, and two individuals were compound heterozygous for two of the ten mutations. The distribution of genotypes is shown in Table 1. A total of 91 individuals were carriers of one or two of the ten *FLG* mutations. Thus, the mutant allele frequency was 0.057, and the carrier rate was 0.111 in the present study. To confirm the reliability of the present real-time PCR-based rapid detection system of *FLG* mutations, the accuracy of genotyping was confirmed by direct sequencing or PCR-restriction fragment length polymorphism (RFLP) of samples obtained from all carriers and selected noncarriers of the null mutations. As a result, the presence of *FLG* mutations was confirmed by direct sequencing or PCR-RFLP in all 93 alleles in which the mutations were detected by the real-time PCR-based system. We performed direct sequencing or PCR-RFLP on 220 alleles (11 individuals, ten mutations) in which no mutation was detected by the real-time PCR-based system, and we confirmed that no mutation was found in any of the studied alleles. These results clearly indicate that the present real-time PCR-based rapid detection system for the Japanese-population-specific *FLG* mutations is a highly reliable screening method for population-specific *FLG* mutations.

In Yakumo town, the prevalence rate of *FLG* mutations was found to be relatively high (11.1%) compared with the data of previous reports (2, 3). We do not know the exact reason, but one possibility is that we studied all the Japanese-population-specific FLG mutations that we have detected for the last 8 years in the Japanese population, whereas the prevalence rates of *FLG* mutations in European studies were mostly evaluated from the data of studies on only a few prevalent mutations, for example, screening only for R501X and 2282del4, or for the five prevalent mutations in the European population. If only the seven mutations reported in the previous study in 2009 (9) had been used in the present study, the prevalence rate of FLG mutations in Yakumo town would have been only 7.7%. In light of this, the higher prevalence rate of 11.1% in the present study might be a reasonable value. On the other hand, we cannot exclude the possibility that the present subjects have skewed genetic backgrounds regarding *FLG* mutations, because many Yakumo residents are descendants of immigrants who moved to Yakumo from a limited area of Nagoya city in central Japan.

According to the present data from a clinical questionnaire given to 816 Yakumo residents, 63 individuals reported having had frequent episodes of watery eyes, runny nose, and sneezing, and they were considered to be putative hay fever patients. Of the 91 individuals with *FLG* mutations, 12 individuals were putative hay fever patients (13.2%), and of the 725 individuals without *FLG* mutations, 51 were putative hay fever patients (7.0%). Thus, *FLG* mutations were significantly associated with putative hay fever (odds ratio = 2.01 [95% CI: 1.027–3.936, $P < 0.05$]; Table 2).

Table 2 Prevalence of history of asthma, watery eyes, and runny nose (n = 820) for the total group and the subgroups of individuals with the combined genotype (n = 91) and without the combined genotype (n = 729)

History	All individuals% (n)	Individuals with FLG mutations% (n)	Individuals without FLG mutations% (n)	OR	95% CI	P-value
Asthma	6.6 (54/815)	10 (9/90)	6.2 (45/725)	1.68	0.792–3.561	0.129
Watery eyes	20.8 (170/817)	22 (20/91)	20.7 (150/726)	1.08	0.638–1.833	0.431
Runny nose	25.9 (211/816)	24.2 (22/91)	26.1 (189/725)	0.90	0.544–1.502	0.403
Watery eyes and runny nose	9.1 (74/816)	14.3 (13/91)	8.4 (61/725)	1.81	0.954–3.451	0.056
Putative hay fever (watery eyes, runny nose, sneezing)	7.7 (63/816)	13.2 (12/91)	7 (51/725)	2.01	1.027–3.926	0.038

Concerning asthma, of the 90 individuals with *FLG* mutations, nine individuals had asthma history (10.0%), and of the 725 individuals without *FLG* mutations, 45 had asthma history (6.2%). Thus, asthma history was not significantly associated with *FLG* mutations (odds ratio = 1.68 [95% CI: 0.792–3.561, P = 0.129]; Table 2). This result, that is, nonsignificant association of general asthma with *FLG* mutations, is consistent with previous data by case–control study (4, 10). However, in the present study, we think that the association between the *FLG* mutations and asthma was maybe not significant, due to the reduced sample size and power.

Weidinger et al. (11) reported that, independent of eczema, *FLG* mutations confer a substantial risk for allergic rhinitis. Contrasting reports suggest that the significant association observed between *FLG* mutations and hay fever may be due to the close association between *FLG* mutations and patients with both hay fever and eczema (10, 12). As for asthma, the significant association between the *FLG* mutations and asthma was thought to be due to the close association between *FLG* mutations and asthma patients with eczema (10–12), although there is a report that suggests a significant association between *FLG* mutations and eczema-free asthma patients (13). In light of this, we tried to perform subphenotype analysis to clarify the connection between *FLG* mutations and hay fever/asthma in the eczema patients and the noneczema individuals. However, in these subphenotype analyses, the sample sizes were too small, and we were unable to obtain reliable data (Data S2). Thus, it is not clear whether the association between *FLG* mutations and hay fever in the present study is due to the close association between *FLG* mutations and hay fever patients with eczema.

A number of case–control studies have addressed the association of *FLG* mutations with asthma and hay fever (2–4, 10, 11). However, the number of studies among the general population is limited, and previous studies were performed only for prevalent *FLG* mutations in each population. In contrast, in the present study, we performed comprehensive screening for almost all the population-specific *FLG* mutations in the general population. In light of this, our present results are noteworthy when we discuss the significance of *FLG* mutations in the pathogenesis of hay fever.

Author contributions

MK, NH, WHIM, HS, and MA contributed study conception and design. MK, TN, NH, YO, OM, SS, HT, and NH contributed data acquisition and analysis. MK, NH, HS, and MA contributed data interpretation. MK and MA wrote the manuscript, and MK, TN, NH, HS, and MA revised it critically for important intellectual content. All authors approved the final version of the manuscript.

Funding

Grants-in-Aid for Scientific Research (A) 23249058 (to MA) and (C) 24591646 (to MK) from the Ministry of Education, Culture, Sports, Science and Technology of Japan.

Conflicts of interest

The authors declare no conflicts of interest.

Supporting Information

Additional Supporting Information may be found in the online version of this article:

Table S1. The sequence of assay probes/primers.

Data S1. Materials and methods.

Data S2. Results: subphenotype analysis.

References

1. McAleer MA, Irvine AD. The multifunctional role of filaggrin in allergic skin disease. *J Allergy Clin Immunol* 2013;**131**:280–291.
2. Rodriguez E, Baurecht H, Herberich E, Wagenpfeil S, Brown SJ, Cordell HJ et al. Meta-analysis of filaggrin polymorphisms in eczema and asthma: robust risk factors in atopic disease. *J Allergy Clin Immunol* 2009;**123**:1361–1370.
3. van den Oord RA, Sheikh A. Filaggrin gene defects and risk of developing allergic sensitisation and allergic disorders: systematic review and meta-analysis. *BMJ* 2009;**339**: b2433.
4. Osawa R, Konno S, Akiyama M, Nemoto-Hasebe I, Nomura T, Nomura Y et al. Japanese-specific filaggrin gene mutations in Japanese patients suffering from atopic eczema and asthma. *J Invest Dermatol* 2010;**130**:2834–2836.

5. Thyssen JP, Linneberg A, Johansen JD, Carlsen BC, Zachariae C, Meldgaard M et al. Atopic diseases by filaggrin mutations and birth year. *Allergy* 2012;**67**:705–708.
6. Nomura T, Sandilands A, Akiyama M, Liao H, Evans AT, Sakai K et al. Unique mutations in the filaggrin gene in Japanese patients with ichthyosis vulgaris and atopic dermatitis. *J Allergy Clin Immunol* 2007;**119**:434–440.
7. Nemoto-Hasebe I, Akiyama M, Nomura T, Sandilands A, McLean WH, Shimizu H. FLG mutation p.Lys4021X in the C-terminal imperfect filaggrin repeat in Japanese patients with atopic eczema. *Br J Dermatol* 2009;**161**:1387–1390.
8. Itou S, Goto Y, Suzuki K, Kawai S, Naito M, Ito Y et al. Significant association between methylenetetrahydrofolate reductase 677T allele and hyperuricemia among adult Japanese subjects. *Nutr Res* 2009;**29**:710–715.
9. Nomura T, Akiyama M, Sandilands A, Nemoto-Hasebe I, Sakai K, Nagasaki A et al. Prevalent and rare mutations in the gene encoding filaggrin in Japanese patients with ichthyosis vulgaris and atopic dermatitis. *J Invest Dermatol* 2009;**129**:1302–1305.
10. Schuttelaar ML, Kerkhof M, Jonkman MF, Koppelman GH, Brunekreef B, de Jongste JC et al. Filaggrin mutations in the onset of eczema, sensitization, asthma, hay fever and the interaction with cat exposure. *Allergy* 2009;**64**:1758–1765.
11. Weidinger S, O'Sullivan M, Illig T, Baurecht H, Depner M, Rodriguez E et al. Filaggrin mutations, atopic eczema, hay fever, and asthma in children. *J Allergy Clin Immunol* 2008;**121**:1203–1209.
12. Marenholz I, Nickel R, Ruschendorf F, Schulz F, Esparza-Gordillo J, Kerscher T et al. Filaggrin loss-of-function mutations predispose to phenotypes involved in the atopic march. *J Allergy Clin Immunol* 2006;**118**:866–871.
13. Li M, Chen X, Chen R, Bao Y, Yao Z. Filaggrin gene mutations are associated with independent atopic asthma in Chinese patients. *Allergy* 2011;**66**:1616–1617.

ARTHRITIS & RHEUMATOLOGY
Vol. 66, No. 12, December 2014, pp 3457–3462
DOI 10.1002/art.38866

BRIEF REPORT

Autoantibodies to DNA Mismatch Repair Enzymes in Polymyositis/Dermatomyositis and Other Autoimmune Diseases: A Possible Marker of Favorable Prognosis

Yoshinao Muro,[1] Ran Nakashima,[2] Yuji Hosono,[2] Kazumitsu Sugiura,[1] Tsuneyo Mimori,[2] and Masashi Akiyama[1]

Objective. **Myositis-specific autoantibodies (MSAs) are useful tools for identifying clinical subsets of patients with idiopathic inflammatory myopathies (IIMs). There have been few reports on antibodies to some DNA mismatch repair enzymes (MMREs) in patients with IIMs. This study was undertaken to determine the frequencies and clinical associations of antibodies to 7 types of MMREs (MLH1, MLH3, MSH2, MSH3, MSH6, PMS1, and PMS2) in patients with IIMs and other systemic autoimmune diseases.**

Methods. **Clinical data and serum samples were collected from 239 Japanese patients with IIMs (147 with adult dermatomyositis, 13 with juvenile dermatomyositis, 57 with polymyositis, and 22 with myositis overlap syndrome). One hundred patients with other diseases, including 40 with systemic lupus erythematosus (SLE), were assessed as disease controls. The presence of anti-MMRE antibodies in serum was examined by immunoprecipitation, enzyme-linked immunosorbent assay, and immunoprecipitation/Western blotting.**

Results. **Anti-MMRE antibodies were found in 15 patients with IIMs and 3 patients with SLE. They were restricted to MLH1, PMS1, MSH2, and PMS2, with simultaneous positivity for more than one of these antibodies occurring in some patients. Nine IIM patients with anti-MMREs also had other MSAs and their associated clinical features. All patients with anti-MMREs were still living at the time of the present analysis.**

Conclusion. **Anti-MMRE antibodies, which often coexist with other MSAs, may be serologic markers for good prognosis in IIMs.**

Idiopathic inflammatory myopathies (IIMs) are systemic autoimmune diseases that mainly affect muscle and/or skin. Various myositis-specific autoantibodies (MSAs) and myositis-associated autoantibodies (MAAs) have been described (1). MAAs have been reported in relation to myositis in overlap syndromes with other autoimmune diseases. In contrast, MSAs are exclusive to myositis, and ≥2 MSAs rarely coexist in a single patient.

DNA mismatch repair is one of several DNA repair pathways conserved from bacteria to humans. The primary function of mismatch repair is to eliminate the mismatch of base–base insertions and deletions that appear as a consequence of DNA polymerase errors during DNA synthesis. In humans, there are 2 sets of mismatch repair enzymes (MMREs), corresponding to homologs of the bacterial MutS and MutL systems (2). The human MutS homologs are MSH2, MSH3, and MSH6, and human MutL homologs include MLH1, MLH3, PMS1, and PMS2.

A 2001 report described the presence of autoantibodies to PMS1 in patients with IIM (3). Autoantibodies to PMS2 and MLH1 were also present in some patients. In 2005, anti-PMS1 and anti-MSH2 antibodies were found in Japanese patients with IIMs (4). In the present study, we evaluated the frequencies and clinical implications of autoantibodies to the 7 types of MMREs in patients with IIM and other autoimmune diseases.

PATIENTS AND METHODS

Patients. Serum samples from 239 Japanese patients (56 male, 183 female) with IIM (147 with adult dermatomyo-

Supported by the Ministry of Education, Culture, Sports, Science, and Technology of Japan (grants 23591618 to Dr. Muro and 23249058 to Dr. Akiyama) and the Ministry of Health, Labor, and Welfare of Japan (grant to Dr. Muro).

[1]Yoshinao Muro, MD, PhD, Kazumitsu Sugiura, MD, PhD, Masashi Akiyama, MD, PhD: Nagoya University Graduate School of Medicine, Nagoya, Japan; [2]Ran Nakashima, MD, PhD, Yuji Hosono, MD, Tsuneyo Mimori, MD, PhD: Kyoto University Graduate School of Medicine, Kyoto, Japan.

Address correspondence to Yoshinao Muro, MD, PhD, Division of Connective Tissue Disease and Autoimmunity, Department of Dermatology, Nagoya University Graduate School of Medicine, 65 Tsurumai-cho, Showa-ku, Nagoya 466-8550, Japan. E-mail: ymuro@med.nagoya-u.ac.jp.

Submitted for publication March 22, 2014; accepted in revised form August 26, 2014.

sitis [DM], 13 with juvenile DM, 57 with polymyositis [PM], and 22 with myositis overlap syndrome) were analyzed for this study. The sera were from 144 patients seen at Nagoya University Hospital between 1994 and 2013 and 95 patients seen at Kyoto University Hospital between 2004 and 2013. They were obtained at the time of diagnosis (except for 2 samples obtained at a later time point from patients with juvenile DM) and were from consecutive patients in most cases (samples from some consecutively diagnosed patients were not available for study). One hundred patients with other autoimmune diseases (40 with systemic lupus erythematosus [SLE], 20 with systemic sclerosis [SSc], 20 with rheumatoid arthritis [RA], and 20 with Sjögren's syndrome [SS]) were assessed as disease controls. All 57 patients with PM and 95 of the patients with adult DM fulfilled the Bohan and Peter criteria (5); 52 patients fulfilled the Sontheimer criteria for clinically amyopathic DM (CADM) (6). The patients with SLE, RA, and SSc met the respective American College of Rheumatology classification criteria for these diseases (7–9). SSc was classified as diffuse cutaneous or limited cutaneous according to the criteria of LeRoy et al (10). SS was diagnosed based on Japanese diagnostic criteria (11). Clinical information was collected retrospectively by medical chart review. The study was conducted with the approval of the ethics committees of the Nagoya University Graduate School of Medical Science and the Kyoto University Graduate School of Medical Science.

Laboratory tests and serologic assays. Serum samples were screened for antibodies against SSA, SSB, U1 RNP, Sm, CENP-B, and double-stranded DNA (dsDNA) using commercial enzyme-linked immunosorbent assay (ELISA) kits (MBL). In addition, anti–Mi-2, anti–transcription intermediary factor 1γ (anti–TIF-1γ), anti–melanoma differentiation–associated protein 5 (anti–MDA-5), anti–nuclear matrix protein 2 (anti–NXP-2), and anti–aminoacyl–transfer RNA synthetase (anti-aaRS) antibodies were investigated by protein and RNA immunoprecipitation (12) and/or immunoprecipitation with recombinant protein (13).

Immunoprecipitation and ELISA using recombinant protein. The full-length complementary DNA (cDNA) clones of 7 human MMREs (Flexi ORF Clone) were purchased from Promega. Biotinylated recombinant protein was produced from the cDNA, using a T7 Quick Coupled Transcription/Translation System (Promega) according to our previously described protocol (13). Briefly, 800 μl TnT Quick Master Mix, 20 μl 1 m*M* methionine, 30 μl biotin-lysyl–transfer RNA, 120 μl water, and 30 μl DNA (1 μg/μl) were mixed and then incubated for 60 minutes at 30°C. Immunoprecipitation was performed using in vitro translation and transcription (TnT) products as previously described (13).

Anti-MMRE antibodies were also tested by antigen-capture ELISA according to our previously described methods (14). Briefly, a 96-well Immobilizer Streptavidin Plate (Thermo Scientific Nunc) was incubated with 1 μl/well of TnT reaction mixture including biotinylated recombinant protein. Wells were then incubated with sera (1:1,000 dilution) and probed with horseradish peroxidase–conjugated anti-human IgG antibody (1:30,000 dilution; Dako). After incubation with SuperSignal ELISA Femto Maximum Sensitivity Substrate (Thermo Scientific Pierce), relative luminescence units (RLU) were determined using a GloMax-Multi Detection System (Promega). Each serum sample was tested in duplicate, and the mean RLU minus background was used for data analysis. The RLU of the samples was converted into units using a standard curve created with a prototype positive serum.

Immunoprecipitation/Western blotting. Immunoprecipitation assays were performed using extracts of the leukemia cell line K562 as previously described (12), with minor modifications. Patient serum (10 μl) was bound to 10 μl of protein G–Sepharose Fast Flow (GE Healthcare Japan) in 500 μl of immunoprecipitation buffer (10 m*M* Tris HCl [pH 8.0], 500 m*M* NaCl, 0.1% Nonidet P40) and incubated for 2 hours at 4°C, followed by washing 5 times with immunoprecipitation buffer. Antibody-coated Sepharose beads were mixed with 100 μl K562 cell extracts derived from 10^6 cells and rotated at 4°C for 2 hours. After 5 washes, the beads were resuspended in sodium dodecyl sulfate (SDS) sample buffer, and samples were fractionated by SDS–polyacrylamide gel electrophoresis followed by Western blotting. Polyclonal antibodies to MLH1, MSH2, PMS1, and PMS2 were purchased from Santa Cruz Biotechnology.

Statistical analysis. Statistical significance was assessed by Fisher's exact test, Mann-Whitney U test, or log rank test, as appropriate. Data were evaluated using SPSS Statistics (IBM). *P* values less than 0.05 were considered significant.

RESULTS

Detection of anti-MMRE antibodies in patients with IIM and other autoimmune diseases. Serum samples from 239 patients with IIM were screened for anti-MMREs using immunoprecipitation with recombinant proteins. PMS1, MLH1, MSH2, and PMS2 recombinants were immunoprecipitated by 10, 9, 3, and 2 sera, respectively, as determined by TnT immunoprecipitation (Figure 1). They were confirmed to react with the corresponding proteins, since the precipitates were recognized by polyclonal antibodies to these proteins in Western blotting (Figure 1). MLH3, MSH3, and MSH6 were not reactive with any sera from the IIM patients, although their recombinants were produced (Figure 1).

In all of the IIM sera, the presence of each of the 7 anti-MMRE antibodies was also examined by ELISA. With positivity defined as an RLU value more than 5 SD above the mean in 20 healthy controls, these analyses demonstrated that all of the sera that were positive for antibodies to PMS1, MLH1, MSH2, and PMS2 by immunoprecipitation were positive by ELISA as well (data available from the corresponding author upon request). As in the immunoprecipitation analyses, no sera were found by ELISA to be positive for anti-MLH3, anti-MSH3, or anti-MSH6 antibodies.

Positivity for antibodies to PMS1, MLH1, MSH2, and PMS2 was also assessed by ELISA in the sera of disease controls and healthy controls (data available from the corresponding author upon request). The only

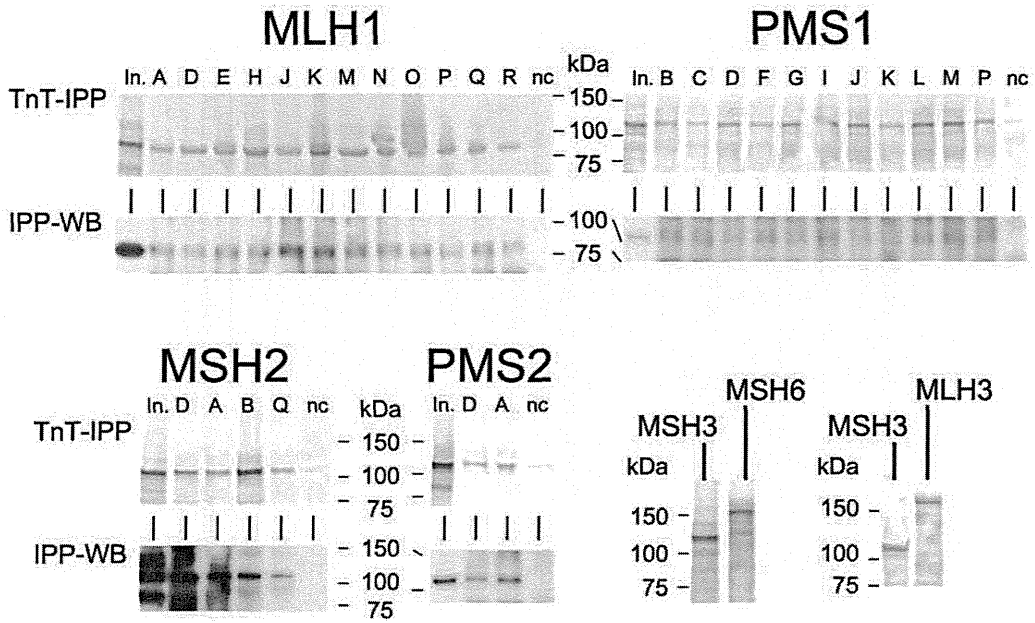

Figure 1. Detection of antibodies to DNA mismatch repair enzyme (anti-MMRE). In translation and transcription immunoprecipitation (TnT-IPP) experiments, biotinylated recombinant MLH1, PMS1, MSH2, and PMS2 were assessed by immunoprecipitation. Recombinant proteins were subjected to 4–20% sodium dodecyl sulfate–polyacrylamide gel electrophoresis (SDS-PAGE) and analyzed by immunoblotting with streptavidin–alkaline phosphatase and substrate. In immunoprecipitation/Western blotting (WB) experiments, immunoprecipitates from K562 cell extracts with human sera were probed with polyclonal antibodies to MLH1, PMS1, MSH2, and PMS2. The input (In.) was half the dose (or a full dose for immunoprecipitation/Western blotting of MLH1), of the biotinylated proteins or cell extract used for the immunoprecipitation assay. Biotinylated recombinant MSH3, MSH6, and MLH3 were also subjected to 4–20% SDS-PAGE and analyzed by immunoblotting with streptavidin–alkaline phosphatase and substrate; no serum samples immunoprecipitated these recombinants. Lanes A–R correspond to anti-MMRE–positive patients shown in Table 1. nc = normal control serum.

positive results in these assays were found in 3 sera from patients with SLE. All 3 SLE sera were reactive with MLH1; 1 was additionally reactive with PMS1, and another was additionally reactive with MSH2. The presence of antibodies to MLH1, PMS1, and MSH2 in these 3 patients with SLE was confirmed by immunoprecipitation/Western blotting (Figure 1).

Longitudinal study of anti-MMRE antibodies coexisting in individual patients. Among a total of 18 IIM or SLE patients with anti-MMRE, 8 were positive for at least 2 types of anti-MMRE antibodies (Table 1). Patterns of reactivity with 4 MMREs (MLH1, PMS1, MSH2, and PMS2) and their combinations were heterogeneous among patients and were not associated with the specific disease or disease subset (data available from the corresponding author upon request). The coexistence of anti-MLH1 and anti-PMS1 antibodies was found most frequently (5 patients). All patients who were positive for anti-MSH2 and/or anti-PMS2 were also positive for anti-MLH1 and/or anti-PMS1.

To further investigate the associations of antibodies to different MMREs, we obtained longitudinal serum samples from 7 patients who were positive for >1 type of anti-MMRE and examined antibody titers by ELISA (data available from the corresponding author upon request). In patient D, who was positive for 4 different anti-MMREs, titers of all 4 decreased similarly over time. Titers of anti-MLH1 changed in parallel to those of anti-PMS1 in patients J, K, M, and P and in parallel to those of anti-MSH2 in patient Q. In patient B, titers of anti-PMS1 changed similarly to titers of anti-MSH2.

Clinical and laboratory profiles of patients with anti-MMRE antibodies. Of the 239 patients with IIM, 15 were positive for at least 1 anti-MMRE antibody: 5 (5.3%) of 95 adults with DM, 3 (5.3%) of 57 adults with PM, 2 (3.8%) of 52 adults with CADM, 2 (15.4%) of 13 juvenile patients with DM, and 3 (13.6%) of 22 adults with myositis overlap (Table 1). The antibody frequency was higher among female IIM patients (15 of 183) than among male patients (0 of 56) ($P < 0.026$). Muscle symptoms and arthralgia were seen in 12 and 10 patients, respectively, while internal malignancy was not found. Among adult patients with DM including CADM, anti-